GEOLOGIC CONTROLS ON RESERVOIR QUALITY OF THE HUNTON AND VIOLA
LIMESTONES IN THE LEACH FIELD, JACKSON COUNTY, KANSAS

by

JOSHUA JAY RENNAKER

B.S., Kansas State University, 2014

A THESIS

submitted in partial fulfillment of the requirements for the degree

MASTER OF SCIENCE

Department of Geology
College of Arts and Sciences

KANSAS STATE UNIVERSITY
Manhattan, Kansas

2016

Approved by:

Major Professor
Dr. Matthew Totten

Copyright

JOSHUA JAY RENNAKER

2016

Abstract

The area of study for this project is the Leach Field, which is located in Jackson County, Kansas. Production in the Leach Field has historically been disappointing, with 388,787 barrels of oil being produced since the field's discovery in 1963 (KGS, 2015). Production of the field has been highly variable, with only 20,568 barrels of oil being produced in the last 20 years. Economic and other concerns that have impacted production and production rates of the field include: low oil prices soon after its discovery, numerous changes of ownership, and lack of significant production infrastructure in the area. Stroke of Luck Energy & Exploration, LLC. has recently purchased the majority of the leases and wells in the Leach Field, and is reestablishing the field as a productive oil field. Plans include: washing down several plugged and abandoned wells, and drill new wells to increase production in the field. The goal of this study was to determine the major geologic factors controlling reservoir quality in the Hunton and Viola Limestone Formations in the Leach Field, so that a future exploration model can be developed to help increase and stabilize the field's overall production. This model was created by applying several testing methods including: well logging analysis, microscope analysis, and subsurface mapping. Based on these results it was determined that the quality of the reservoir rocks is controlled by the degree of dolomitizaiton in both formations. Reservoir quality is as important as structure in determining well productivity in the Leach Field.

Table of Contents

List of Figures

List of Tables

Chapter 1 - Introduction

1.1 Introduction to the Leach Field

The Leach Field is located in west central Jackson County, Kansas in the Grant Township, as seen in Figure 1. Jackson County is located in the northeast portion of the state and is situated on the western edge of the Forest City Basin near where the basin meets the Nemaha Anticline. The field falls into a northeast trending line of producing fields that run parallel to the trend of the Nemaha Uplift. Larger more developed fields along this trend include: Davis Ranch, John Creek, McClain, Newbury, and Wilmington Field. Collectively these fields have produced 22.5 million cumulative barrels of oil to date (KGS, 2016). Through the same trend many smaller, less developed fields with limited production can be found, including the Leach Field. The Leach Field is located in Sections, 14, 15, 21, and 22 of Township 7S and Range 13E. The nearest surrounding production includes the Casey Field and the Soldier Field. The Casey Field is located six miles to the west and has produced approximately 181,162 barrels cumulatively out of the Viola Limestone. The Soldier Field is located four miles north, with historical production of 21,833 barrels produced from the Hunton and Viola Formations. The Soldier field was recently the focus of a research project with similar goals (Jensik, 2013), and the results from this study are now being realized, with the last three years production totaling 18,817 barrels, which equates to 86% of the field's total production. The Leach field study area was selected with the suggestion of Kansas State University Department of Geology alumni George Petersen, which he believed was underdeveloped.

Figure 1 - Location of study area with respect to major oil fields and provinces of Eastern Kansas. Unnamed triangles represent Kimberlites. (Jensik, 2013)
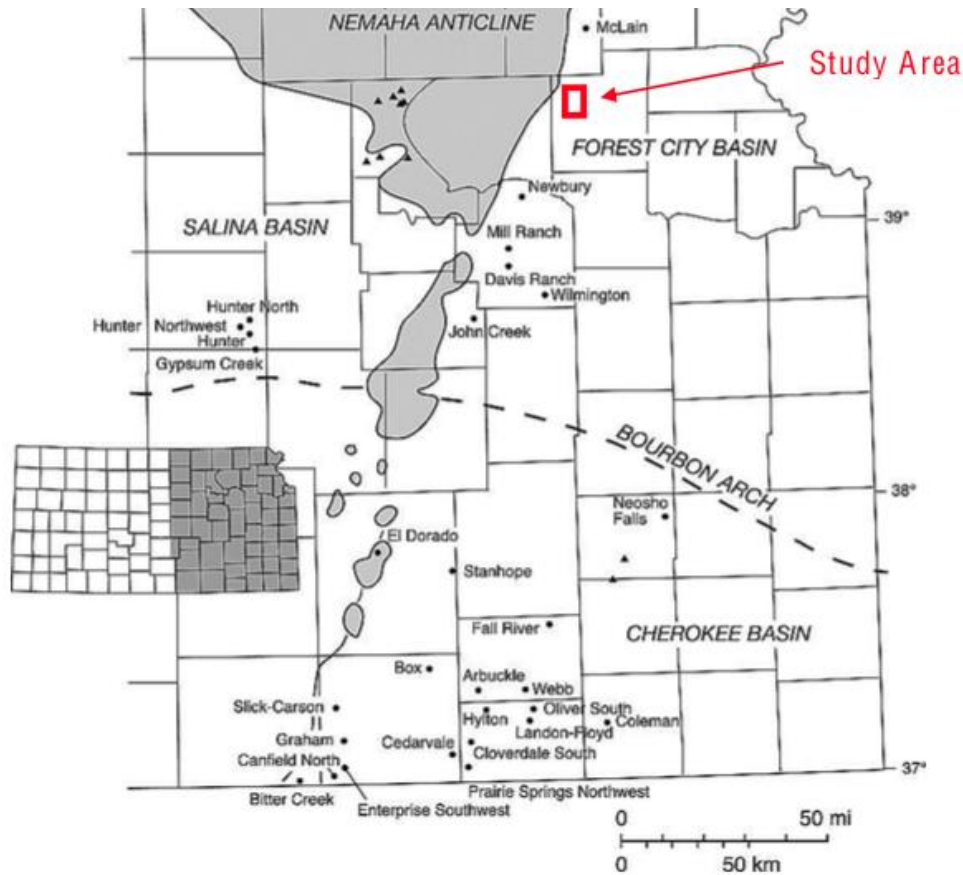
1.2 Leach Field History

The Leach Field was discovered in late 1963 with a wildcat well, Leach 1, and the field's production has been highly variable as a result of numerous changes of ownership, low oil prices, and lack of infrastructure in the area. In the years following the success of the wildcat well the approximately six hundred acre field was leased sporadically by three separate companies, the Phillips Petroleum Company, the Anschutz Oil Company, and the Eureka Drilling Company. The field was orderly developed on forty acre spacing by these three companies, and by the end of the next year there were fifteen wells completed into the Hunton Formation, four wells completed in the Viola Formation, and one disposal well drilled into the Maquoketa Shale Formation. In 1966 Phillips Petroleum Company sold its Leach Field assets to

G.L. Reasor, an independent producer, and Anschutz Oil Company sold its assets to Union of Texas. Soon after taking ownership of a portion of the field, Mr. Reasor fell ill and remained in a coma for an extended period of time until his death, this resulted in his portion of the field being neglected and the wells were eventually temporarily abandoned. For this reason the field had unusually low production numbers from 1968 through late 1970. Following the passing of Mr. Reasor, his assets were purchased by Eureka Drilling. Eureka Drilling also purchased Union of Texas assets, focusing on acquiring the remainder of the Leach Field, which placed the field under one management for the first time in the field's history. Eureka made an effort to reestablish some of the wells that had been shut in for years and an increase in annual field production can be seen on the field production charts. In 1972 oil prices fell to a low price of $1.60 per barrel, and the demand was very low for heavy crude. As a result the Eureka Drilling company reduced production and much of the original equipment was sold. In 1977, the field was acquired by D.W Barnes, and was granted stripper well classification from the Kansas Corporation Commission. Permission was given to infield drill the field on ten acre spacing. After several years of operating the field, D.W Barnes lost the field to his financier. In 1984 the field was once again sold to a newly formed company, the Leach Production Company. Field ownership from 1985 to 2003 is somewhat of an unknown with little to no oil production occurring in those years. In 2003 Elk Oil Enterprises, LLC. acquired partial ownership of the field and produced small amounts from a few wells until 2014. In 2014 Ken Walker and Stroke of Luck Energy and Exploration, LLC began purchasing the field in hopes of restoring the Leach Field production. Field history prior to 1985 was documented in a proprietary report by the Hodgden Oil Company (Hodgden, 1985).

1.3 Paleogeography and Stratigraphy

The Forest City Basin is defined as both a structural and topographic basin that began forming structurally in the late-middle Ordovician time, contemporaneously with the formation of its southern barrier, the Chautauqua arch in southeastern Kansas (Wells, 1987). After deposition near the end of the Mississippian period, the basin was uplifted and gentle folding occurred. The principal fold being the Nemaha anticline, which extends from southeast Nebraska across Kansas into central Oklahoma, Figure 2. At the same time as basin uplift the exposed rocks were subjected to exposure, which eroded these basinal units down to nearly sea level (Lee, 2005). Sedimentation resumed with the advancement of the Pennsylvanian sea, which filled the entire basin, resulting in thicker deposits accumulating in lower areas of the basin than on the higher elevations surrounding (Lee, 2005). After the seas receded, the Nemaha Uplift became active, which resulted in Mississippian rocks that had been nearly flat to become warped downward, forming the Forest City Basin. Figure 3 displays the north-northeast trend of convergence between the basin and anticline, in which many producing oil fields can be found running parallel to the eastern flank of the anticline. The trend can be traced south from the northern Kansas border through the counties of Nemaha, Jackson, Pottawatomie, Wabaunsee, and Morris. In the Forest City Basin, echinoderms, brachiopods, and bryozoans in the upper part of the Viola limestone formation suggest deposition on a shallow, open-marine shelf in waters a few meters to a few tens of meters deep (Caldwell and Boeken, 1985). Areas of planar and cross-stratified grainstones and packstones of the lower Viola suggest deposition in shallower, more agitated, marine waters (Caldwell and Boeken, 1985). These two factors were important for this study, because they can contribute to the amount of porosity found in a petroleum reservoir. Allan and Wiggins, (1993) evaluated the quality and characteristics of dolomite and limestone

reservoirs around the world, and they found that dolomite reservoirs also hold their original

porosity better at greater depths than limestones, Figure 4. For this study the Hunton and Viola

Limestone formations were of geologic focus due to the formations historical, current, and

potential oil production.

Figure 2 - Areas of the Forest City and Cherokee Basin, with the Nemaha anticline, which extends across Nebraska, Kansas into Oklahoma (Lee, 2005).
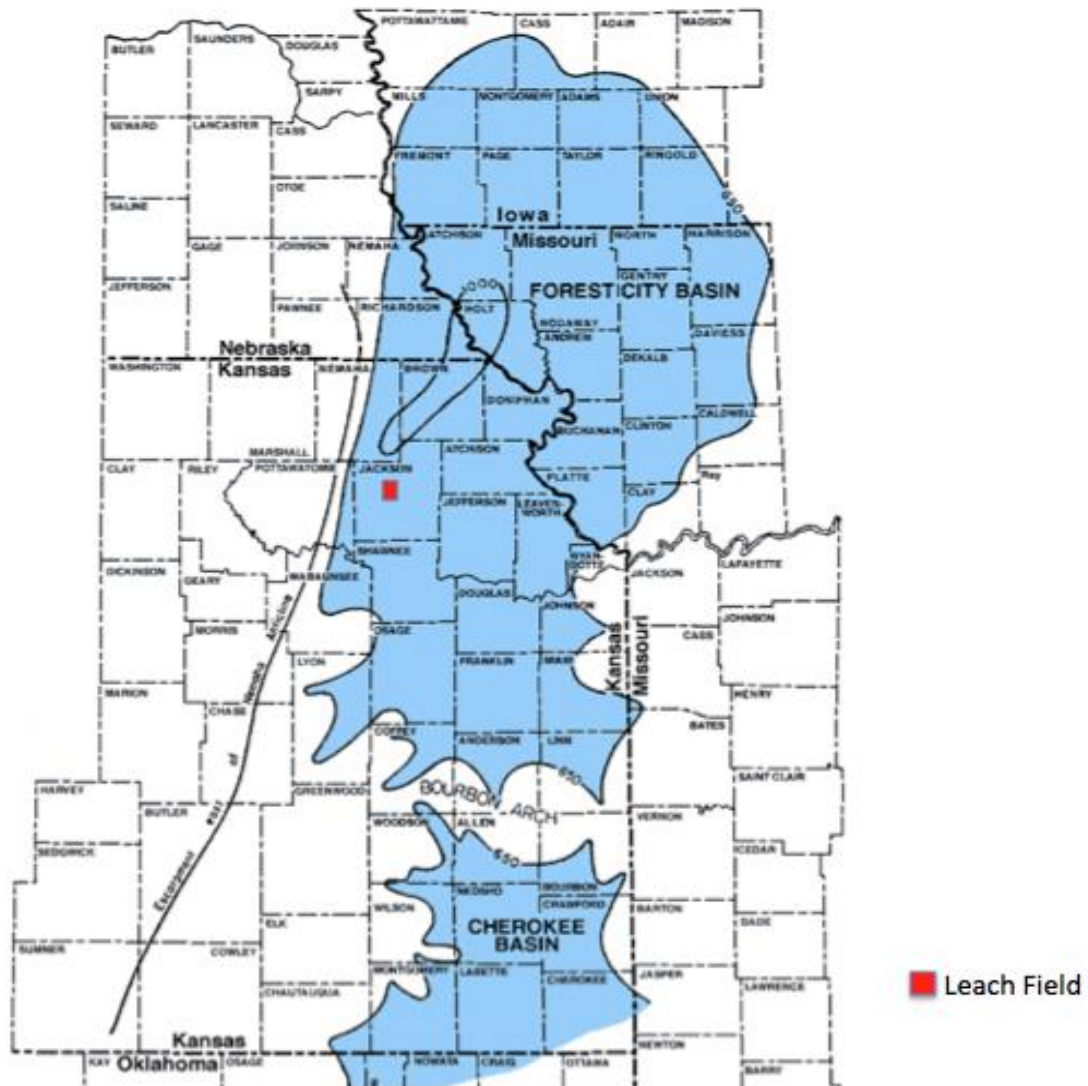
Figure 4 - Trend of producing oilfields along the western edge of the Forest City Basin. (KGS, 2016)
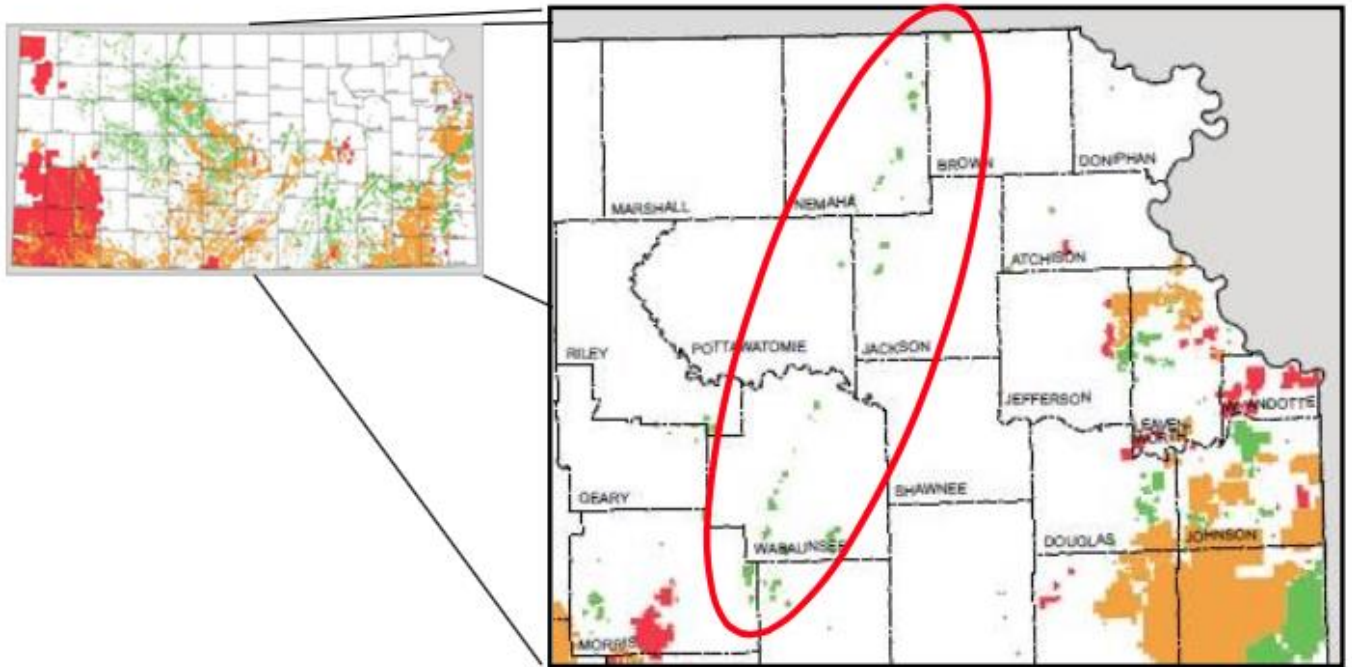
Figure 3 - Progressive loss of porosity with depth (Allen and Wiggins, 1993)
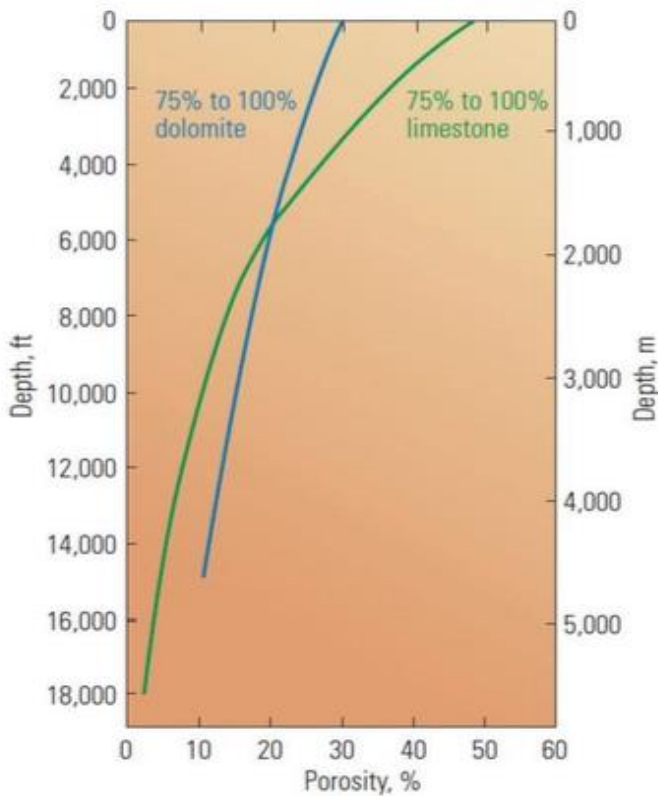
Hunton Group

The Hunton Group is a massive limestone and dolomitic formation of Silurian and Devonian age, Figure 5. The Hunton in the Leach Field is approximately 485 feet thick and is found at a drilling depth of 2,654 feet to 2,774 feet below the surface (Hodgden, 1985). After deposition, the top of the Hunton was exposed and weathered before the deposition of overlying Kinderhook Shale Formation could occur, this allowed for an increase in vuggy porosity near the top of the formation. The fact that the top of the formation has greater porosity due to weathering, results in the Hunton being the main producing reservoir in which most producing wells in the field are drilled. Additional porosity was added to the formation in the form of fractures that were a result of anticlinal folding of the structure (Hodgden, 1985).

Viola Limestone

The Viola Limestone is of Ordovician age and is composed of fine to coarse-grained limestones and dolomites that can contain variable quantities of chert, but in this northern Kansas region it is composed mostly of dolomite (Bornemann, 1982). In the Solider field, four miles to the north of the Leach Field, the Viola is believed to be composed of approximately 95% crystalline dolomite (Jensik, 2013). Porosity types vary across the formation but intergranular, vuggy, moldic, and fracture porosity are common throughout (Newell et al, 1987). In the Leach Field, the Viola Formation is typically found with a thickness of approximately 100 feet (Figure 5), and can be encountered at a drilling depth of 3,211 feet to 3,322 feet below the surface (Hodgden, 1985). Much like the Hunton Formation, historical production from this unit is typically found near the top of the formation where dolomitization is greatest. This dolomitization is thought to have occurred in a freshwater-marine phreatic mixing zones, Figure 6. The result of this alteration is significant increase in the original porosity and permeability of the limestone/dolomite. The

formation is overlain by the Maquoketa Shale with an angular unconformity between the two as a result of the erosion. Major fields in the Forest City basin are almost all structural traps that produce from the Viola Limestone (Newell et al, 1987).

Figure 5 - Stratigraphy of the Forest City Basin, with Hunton and Viola highlighted (Modified from Lee, 2005)
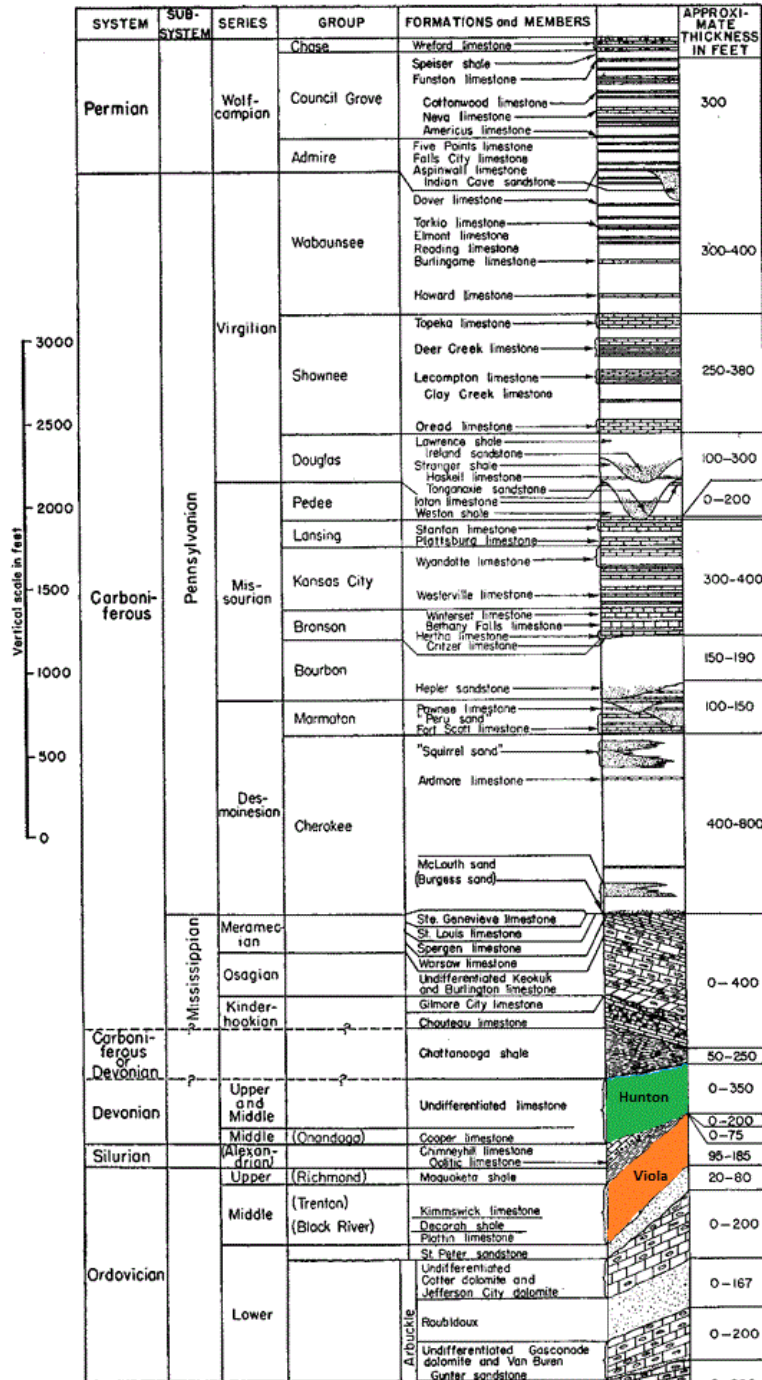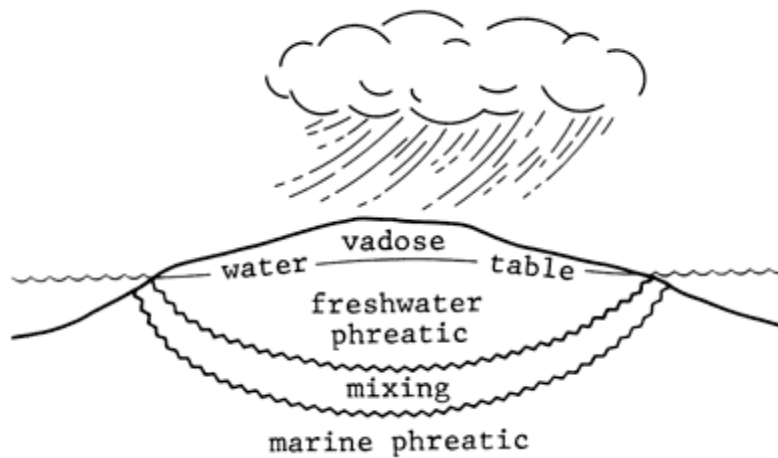
Figure 6 - Idealized shallow-subsurface digenetic environments, not to scale. Dolomitization takes place in the freshwater-marine mixing zones (Caldwell and Boeken, 1985).

1.4 Importance and Previous Studies

The Hunton and Viola Limestone formations are proven hydrocarbon producers in Kansas over the last 100 years. It is estimated that 11% of all oil production will come from Ordovician and Devonian age formations (Adler, 1971). In 2004, the Kansas Geological Survey published a report that estimated the cumulative Kansas oil production from the Viola Formation to be 275 million barrels (Lee, 2005). The Hunton and Viola Limestone formations are very important reservoir formations due to the fact that they are dolomitized, the most important consequence of replacement dolomitization is an accompanying increase in porosity. Dolomitized of formations typically make better oil and gas reservoirs than limestones, and are important in oil and gas exploration because they make up some of the largest reservoirs in the world (Mishari, 2009). Exploration efforts targeting specifically dolomitized reservoirs have been successful, and it is estimated that 50% of the world's carbonate reservoirs are dolomitic in nature (Warren, 2000). A previous reservoir study on the Soldier Field, (Jensik, 2013) which is

located four miles to the north of the Leach Field, had similar research aims as this study. Jensik, (2013) concluded that production in the area is controlled by a combination of both structural position and dolomite crystal size, which was caused by secondary digenesis in freshwater-marine mixing zones. Results of the research are now being realized with the last three years of production of the Soldier Field totaling 18,817 barrels, which equates to 86% of the field's total production since its discovery in 1964.

Chapter 2 - Dolomitization and Porosity Types

2.1 Dolomitization

An estimated 80% of all the oil and gas that will be recovered from carbonate reservoirs will be produced from dolomite or dolomitic limestones (Blatt, et al, 1972). Dolomite, $Ca,Mg(CO_3)_2$ is found in sedimentary basins and is often formed by post-depositional alteration of calcite by magnesium-rich groundwater. In this process magnesium ions from the water replace calcium ions in the calcite and the availability of magnesium (Mg) fluid facilitates the conversion of calcite ($CaCO_3$) to dolomite ($Ca,Mg(CO_3)_2$) (Mishari, 2009). Dolomitization can completely alter a limestone into a dolomite, or partially alter the rock to form a dolomitic limestone. The most important result of dolomitization is the increase in porosity of the rock. Dolomite has a more compact crystal structure than calcite, so total dolomitization of a limestone rock should result in a porosity increase of 13%, barring any subsequent compaction or cementation (Nurmi and Standen, 1997). Study results have shown that planar grains of dolomite create polyhedral pores (Nurmi and Standen, 1997). Consequently, as the dolomite rhombs develop they produce sheet pores and throats rather than tubular pores throats that characterize limestones (Figure 7). These sheet pores and throats allow for greater fluid flow between the rhombohedral crystals and increase the effective porosity of the rock. For this reason, dolomite formations make ideal petroleum reservoirs (Blatt, et al, 1972).

Figure 7 - SEM image of dolomite replacement. Dolomite rhombs (green) growing replacing original calcite (blue) that was high in magnesium (Nurmi and Standen, 1997).
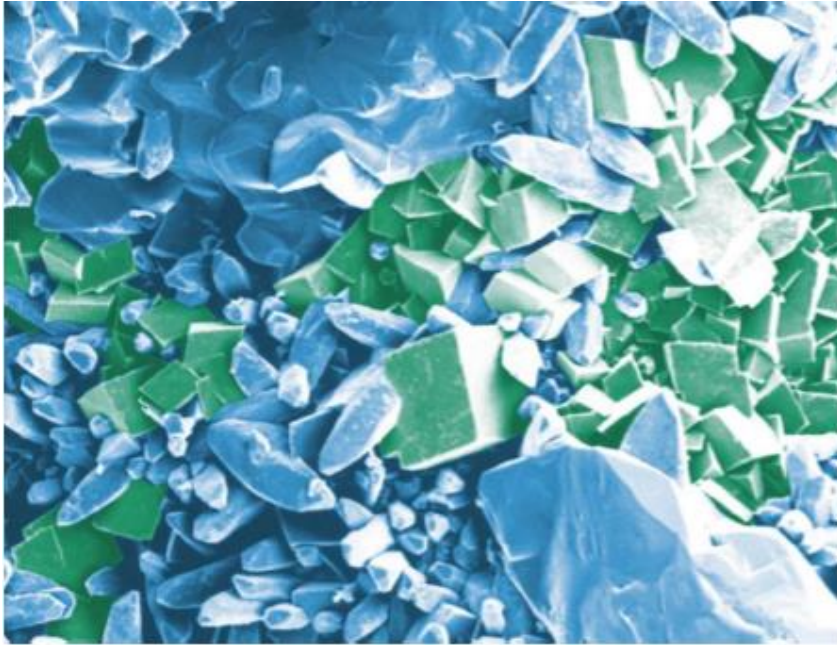
2.2 Carbonate Porosity Types

Porosity controls the availability of space within a formation to store hydrocarbons, which is obviously important to the petroleum industry. Porosity is essentially the volume of void space within a rock, and in a petroleum system directly reflects the potential volume of hydrocarbons the rock can retain. Pore systems play an important role in determining the quality of a reservoir, therefore the ability to identify different types of porosity are important for reservoir studies. Porosity types used in this study will be based on definition defined of Choquette and Pray, (1970). They outlined 15 different types of possible carbonate porosities (Figure 8);

**Figure 8 - Carbonate porosity types (Scholle and Ulmer-Scholle,
2003, modified from Choquette and Pray, 1970)**
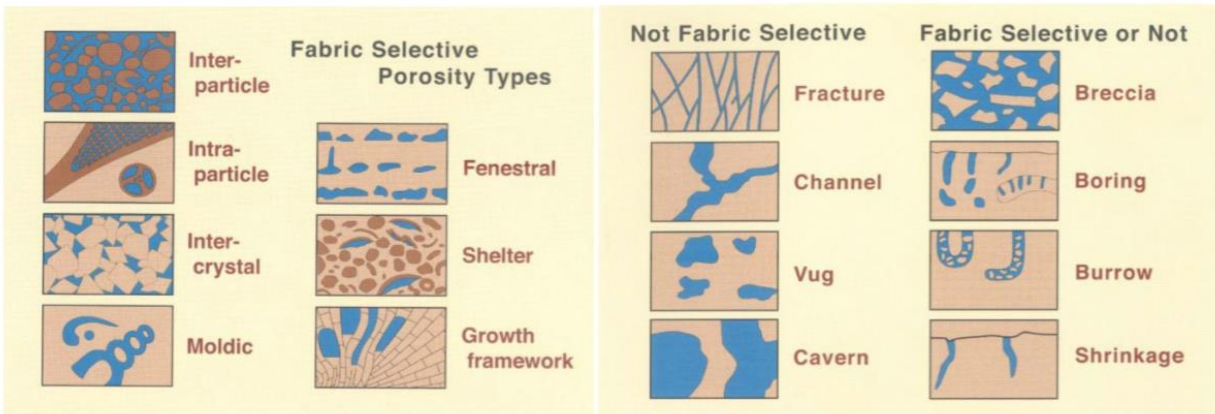
Fracture: porosity is formed by fracturing. "Fracture porosity generally is used for porosity

occurring along breaks in a sediment or rock body where there has been little mutual

displacement of opposing blocks." Carbonate rocks fractures may originate in a several different

ways. The most common origination is due to tectonic deformation, but may also result from

collapse or slumping due to dissolution (Choquette and Pray, 1970). Fractures are important in

reservoir rocks because they connect pores, creating permeability that may not have been present

originally.

Intercrystalline: porosity occurs between crystals of similar or equal size, which have formed by

mineral recrystallization or dolomitization. This occurs as fluid chemistry changes within the

rock, the chemistry can change as layers are deposited. Fluid chemistry can begin changing early

in deposition if the limestone is influenced by meteoric water. It can also be caused by an

unconformity, as well as undergo change late in burial due to hydrocarbon maturation (Blatt, et

al, 1972).

Vuggy: porosity can be described as irregular holes that can cut across grains and cement

boundaries within the rock. Vugs and vuggy porosity are the most common porosity type

descriptions used by geologist when referring to carbonates. Choquette and Pray, (1970) define a

vug as a pore that (1) is somewhat equant, or not markedly elongated, (2) has a diameter greater than 1/16 mm (and visible to the unaided eye), and (3) is not fabric selective. Vuggy porosity is dominantly a secondary porosity and most often occurs because of dissolution.

Moldic: porosity is a secondary process in which grains are removed by dissolution. In order for this process to occur there needs to be a distinct difference in solubility between the grains and the framework (Choquette and Pray, 1970). Moldic porosity can create good permeability if pores are interconnected.

Chapter 3 - Methods and Analysis

Analytical methods employed for this study included: well log analysis, petrographic analysis using a combination of binocular microscope, polarizing microscope analysis of well cuttings, scanning electron microscope and subsurface mapping using IHS Petra® software. These methods were used to determine the reservoir properties controlling oil production in the Leach Field.

3.1 Well Log Analysis

An assembly of well logs for the Leach Field were collected from the Kansas Geological Survey, Stroke of Luck Energy, LLC, and the Walter's Digital Library by the Kansas Geological Society. In order to correctly predict the sample depth that contains samples of interest the lag time was estimated from the log data and drill time date. The formation tops of interest were picked from well logs based on interpretations of log signatures, such as the gamma ray curve, neutron curve, density curve, and induction curve. Because Jackson County lacks an established type log, the identification of formation tops was challenging. The tops were picked based on available completion reports, geologist reports, and a few well logs identified with the assistance of Mr. Petersen. Analysis of well logs for selected wells in the field each allowed for the creation of subsurface maps via IHS Petra® for both the Hunton and Viola Formations.

3.2 Binocular Microscope

Due to an absence of drill core through the Hunton and Viola Limestone formations in the field, drill cuttings were examined in this study. Wells for investigation were selected using three key criteria: 1) the well had to have cuttings available, 2) the wells needed to have additional data available (well logs, scout cards, completion cards), and 3) the well needed to have a record of historical production to serve as an indication of how the reservoir formation

produced in that location. Nine boxes of drill cuttings from separate wells were collected from the Kansas Geological Survey Well Sample in Wichita, Kansas. All well cuttings were first examined using a binocular microscope and handpicked for thin section work. Viewing the cuttings with a binocular microscope gave a sense of which pieces to mount based on: confirming the presence of limestone/dolomite rock, size of cutting, availability of a flat mounting surface, porosity type present, , as well as if any oil staining is present. Using the estimated sample lag time that was determined during well log analysis, samples were accurately selected to represent the producing formations. There is a distinctive dark shale directly above both of the target formations, (Hunton and Viola Limestones), which made picking the correct samples easier.

3.3 Creating Thin Sections

A total of 70 samples were collected at five foot intervals from the nine wells, and thin sections were created for each. Drill cuttings that were selected via well log analysis and handpicked under the binocular microscope were mounted on glass slides using Petropoxy®. The Petropoxy® was impregnated with blue dye so that images of the cuttings could be taken and processed through the ImageJ software to calculate approximate porosity. The porosity in the cuttings was filled with epoxy by submerging samples in epoxy and using a vacuum pump to remove air, which forces the impregnated epoxy into the void spaces of the cuttings. The samples were then placed on a glass slide, aligned to have most surface area glued directly to slide and once again placed under a vacuum to remove possible air bubbles from the epoxy. The slide was then placed on a hot plate to allow the epoxy resin to harden. Once the hardened slide was cooled it was sanded to a thickness of approximately 30 microns on a water cooled brass disk rock grinder. The samples were then polished on a thin section polishing machine using

silicon carbide sandpaper to buff out small scratches and imperfections so that the thin sections would have near perfect finish for microscope work. Refer to Appendix A for more complete instructions for thin sample preparation.

3.4 Petrographic Analysis

Each thin section was examined under a petrographic microscope to document porosity types present, changes in crystal shape and size, and oil staining. The crystal size and shape descriptions were based on Scholle and Ulmer-Scholle, (2003). Photomicrographs were taken of each slide to be used in porosity determination with ImageJ software.

Figure 9 - Defining crystal size (Scholle and Ulmer-Scholle, 2003)

3.5 Scanning Electron Microscope Imaging

Upon completion of binocular microscope, petrographic analysis, and selected thin sections were sent to the University of Kansas for Scanning Electron Microscope work. The SEM produces images of a sample by scanning it with a focused beam of electrons. These electrons interact with atoms within the sample, which reflect back to the detector to produces various signals. These signals allow the machine to create high-resolution optical images of the samples surface. Figure 7 is an image of Nurmi and Standen, (1997) in which they are examining the dolomite replacement in limestones. This analytical method will aid this study in determining

the amount or degree of dolomitization that has occurred in these cuttings, which greatly influences porosity of the rocks.

3.6 Porosity Determination using ImageJ Software

Photomicrographs were processed to determine the average porosity of cuttings using ImageJ. ImageJ is a fast and efficient method developed to measure the total optical porosity of thin sections that have been impregnated with blue epoxy (Grove and Jerram, 2011). What made the ImageJ approach attractive was that the entire ImageJ process requires no specialized equipment and the software is free to download. Adobe Photoshop® was used to prepare the digital images in the correct format, an 8-bit paletted.bmp file. Once images were formatted correctly, they were analyzed in the ImageJ software and porosity was calculated. Refer to Appendix B for step by step instructions on using ImageJ software to calculate porosity from photomicrographs.

3.7 Petra® Mapping Software

A database of well information was constructed from all data collected from the Kansas Geological Survey, well logs, and scientific testing methods. The data base was then imported into Petra® Mapping software, which is made available on an academic license to Kansas State University from IHS, Inc. This software was used to construct a current base map of the field with oil wells, injection wells, and abandoned wells clearly marked. Structure maps of the Hunton and Viola Limestones were generated in an effort to illustrate the structure of the subsurface. It was anticipated that structure maps would display how structural highs control oil and gas production in the Leach Field. Additional maps were constructed to show the distribution of reservoir properties across the field, including porosity estimates for well cuttings of selected wells.

Chapter 4 - Results

4.1 Subsurface Mapping Results

The following maps were created to determine how different attributes control production. Figure 10 is a current base map of the field with oil wells, injection wells, and abandoned wells clearly marked. Figures 11 & 12 are structure maps of both the Hunton and Viola Limestones. Figure 13 shows the location of wells examined in thin section. Figure 14 displays the overall formation porosity estimates for the wells examined using the ImageJ software.

Figure 10 - Leach Field base map.
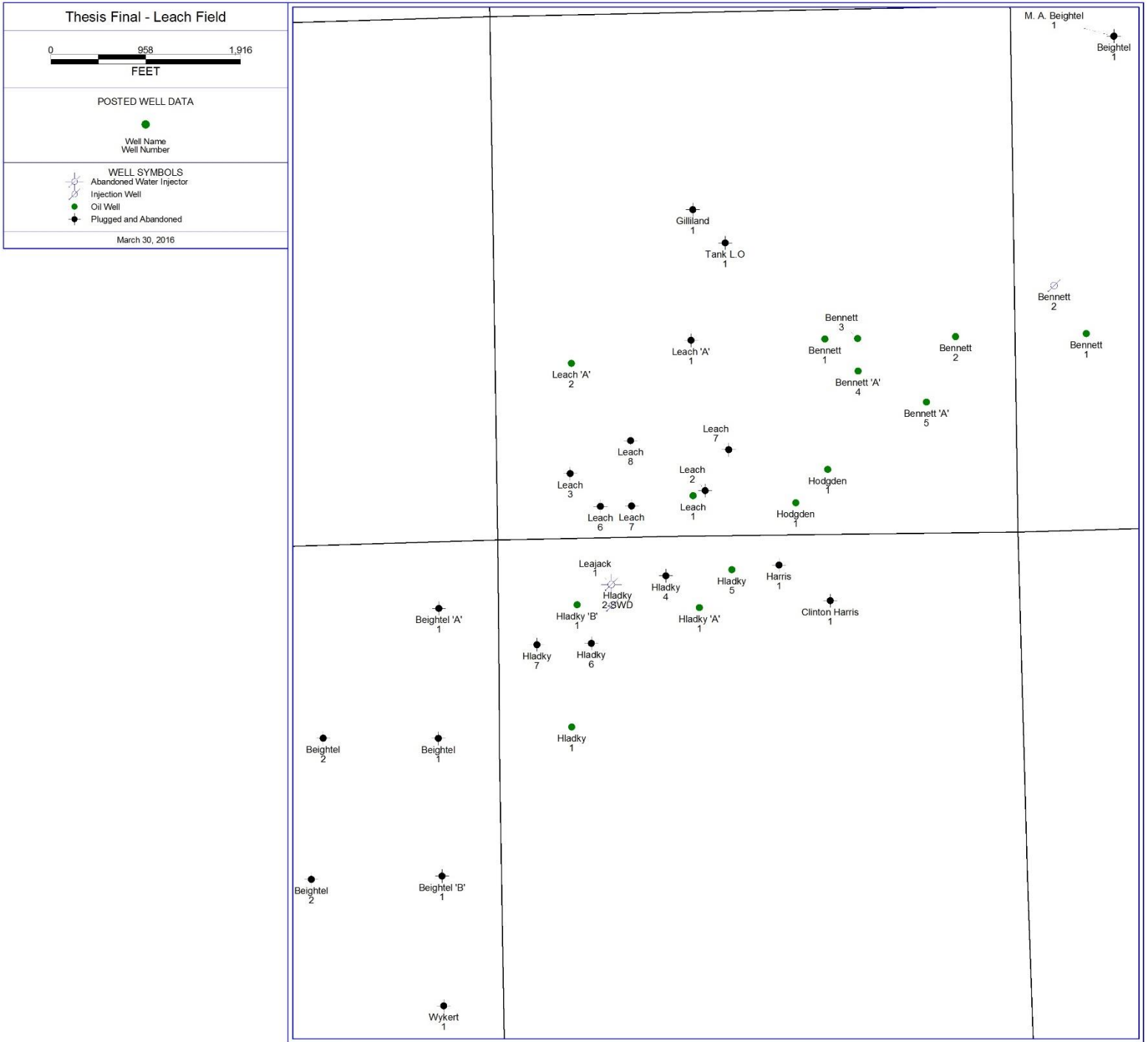
Figure 11 - Hunton Limestone Top, mapped on 20 foot intervals.

21
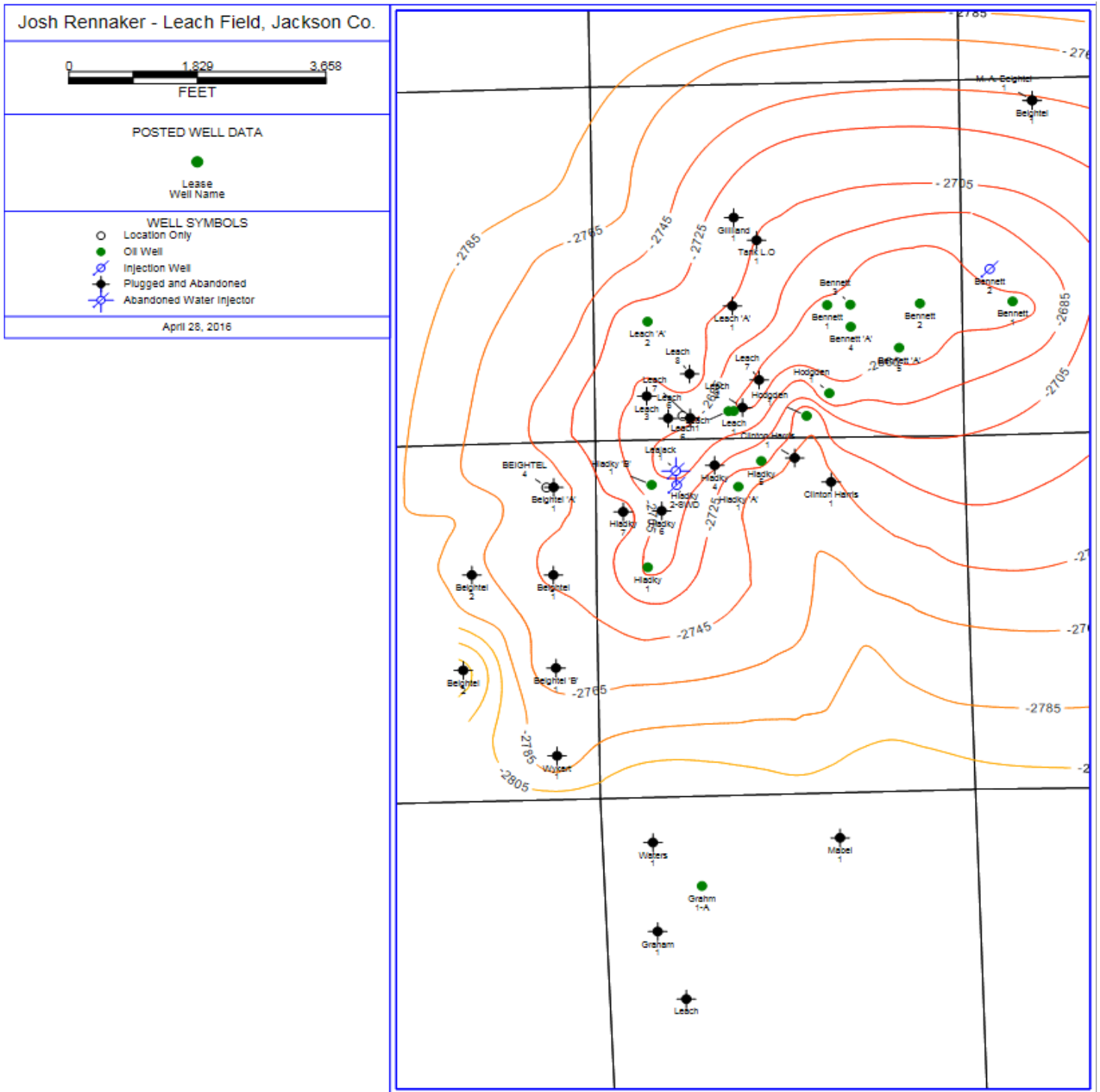
Figure 12 - Viola Limestone Top, mapped on 10 foot intervals.
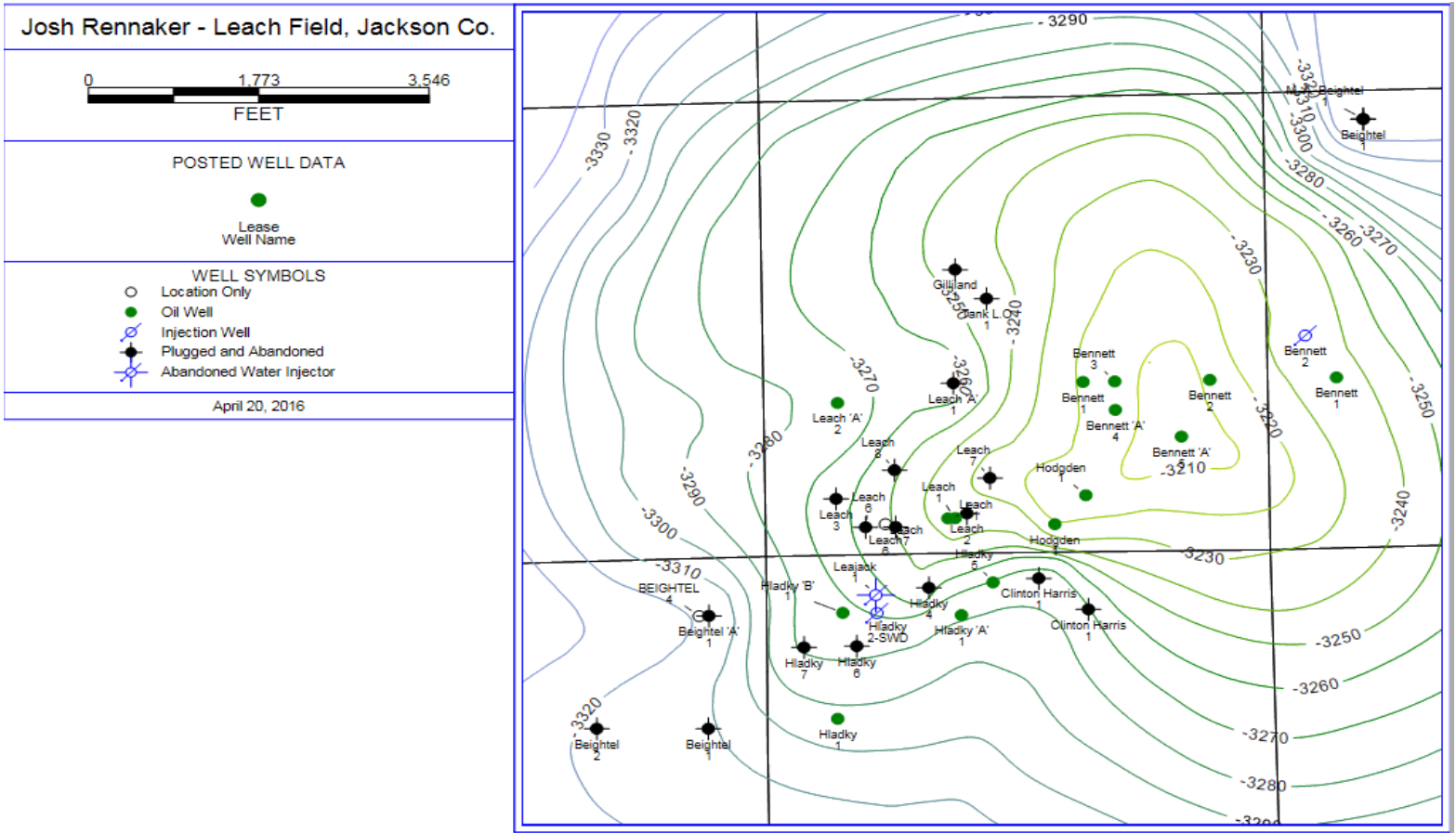
Figure 13 - Thin Section base map.
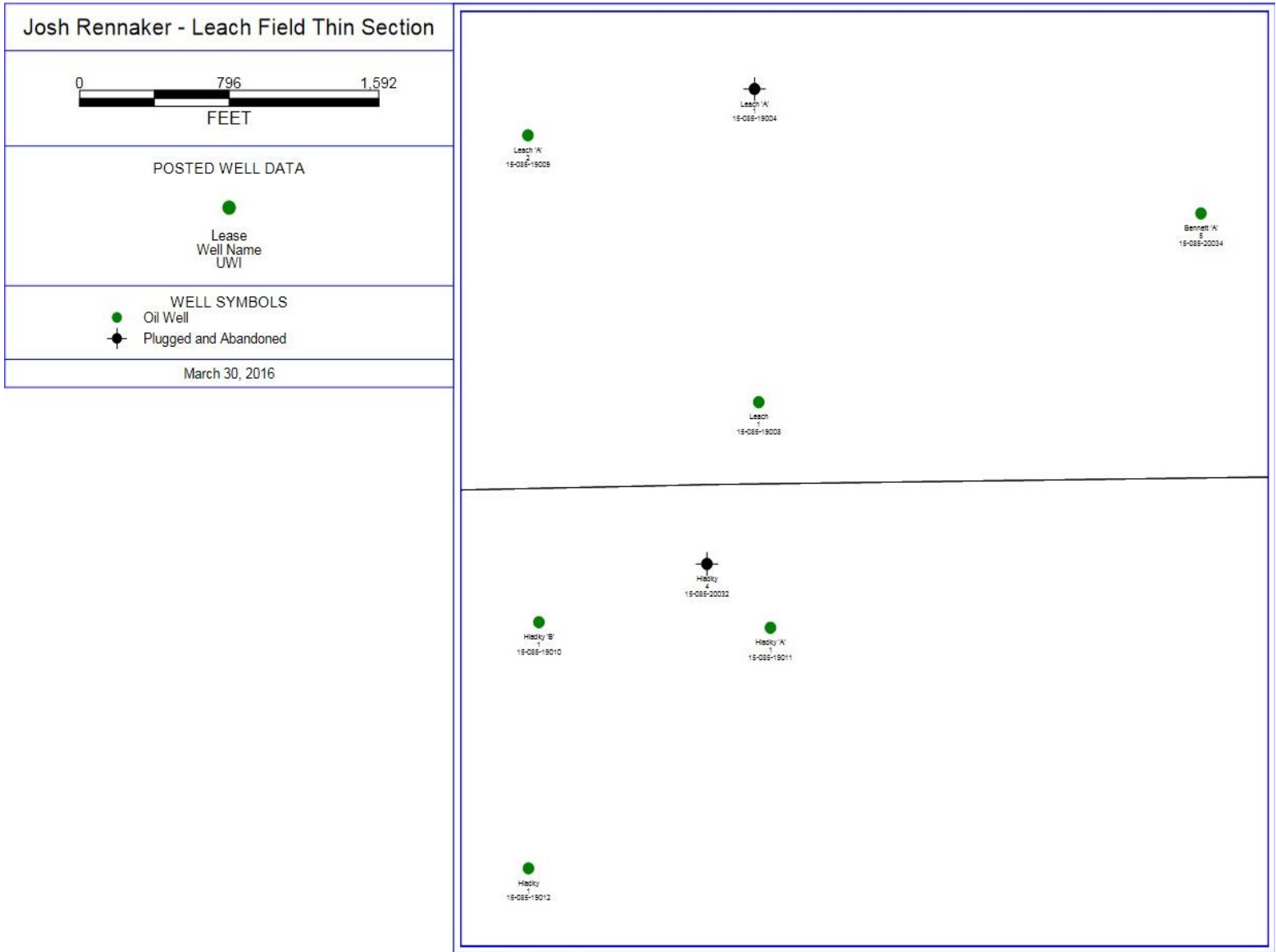
Figure 14 - Overall formation porosity estimates for the wells examined using the ImageJ software.
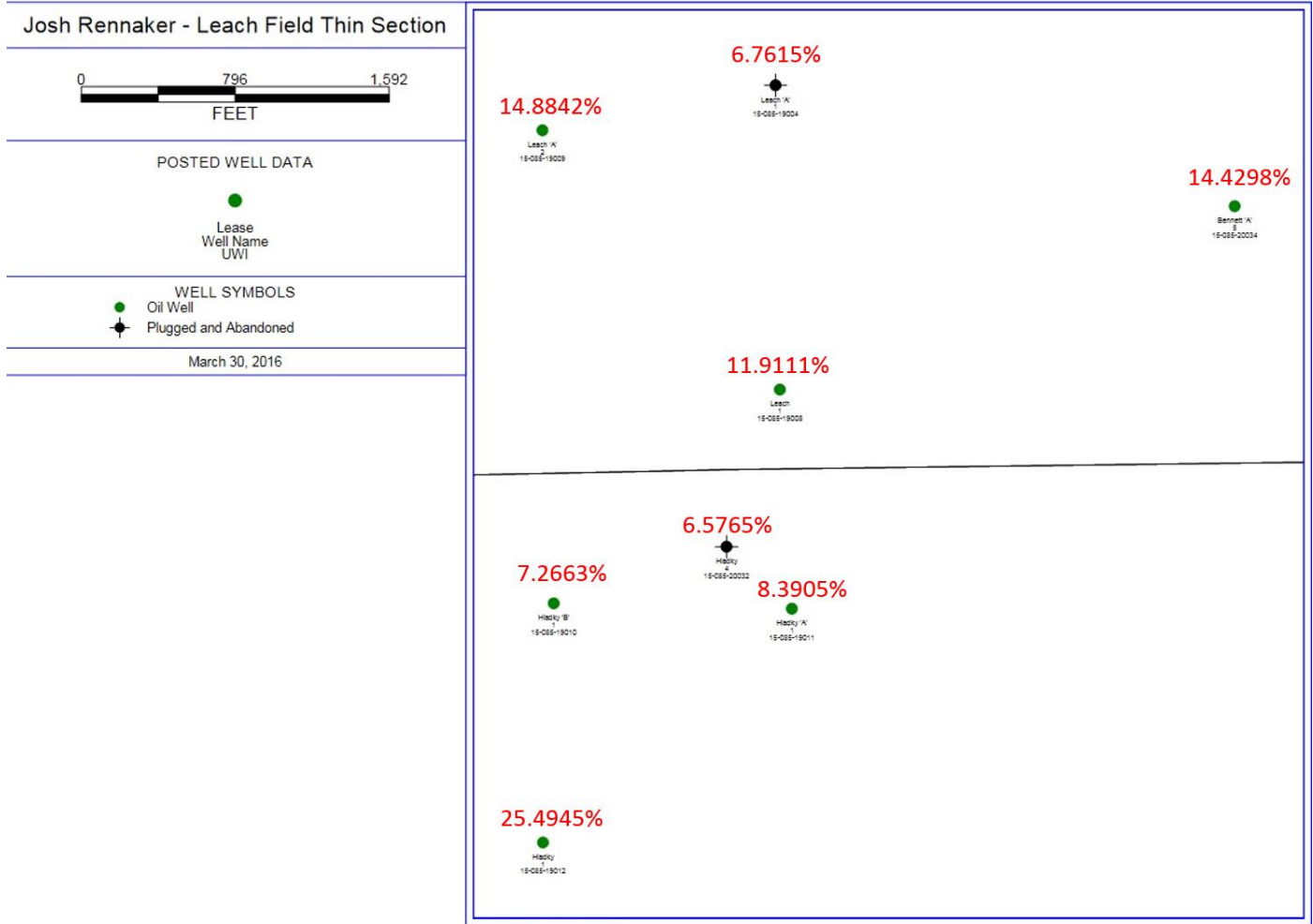
4.2 Petrographic Analysis Results

Table 1 lists the results of drill cutting examination in thin sections under a petrographic microscope. Throughout the petrographic analysis process photomicrographs were taken of each slide. Table 2 displays these images under 10x magnification in both plain polarized light, which will be used in porosity calculation with ImageJ software, and in cross polarized light.
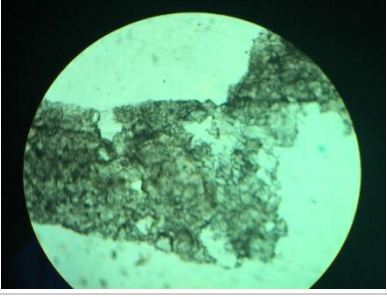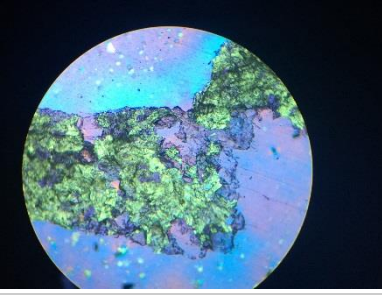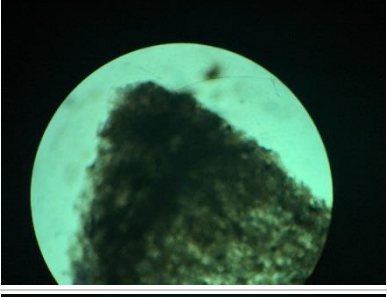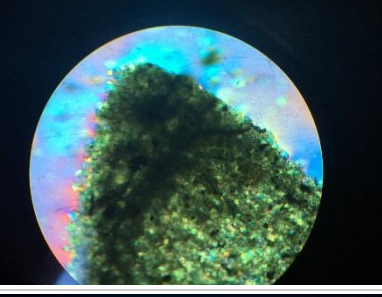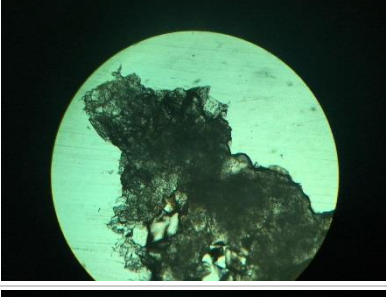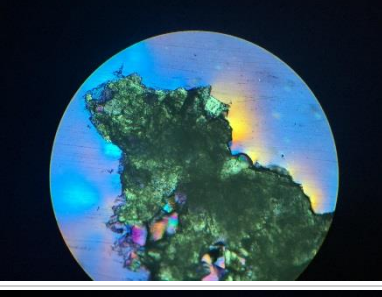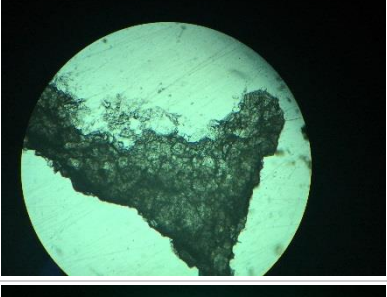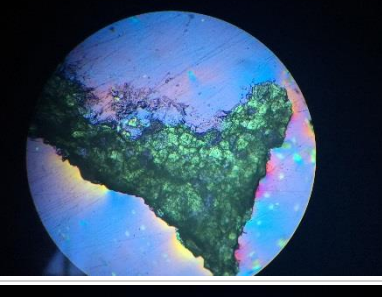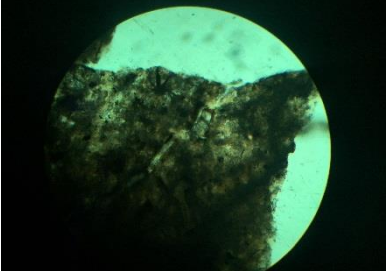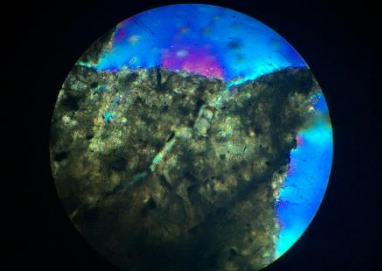
Table 1 - Petrographic Analysis Results
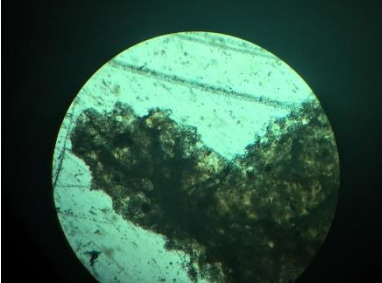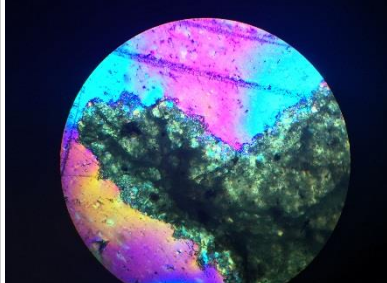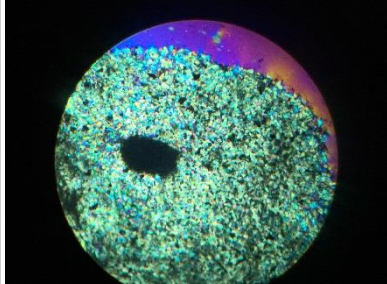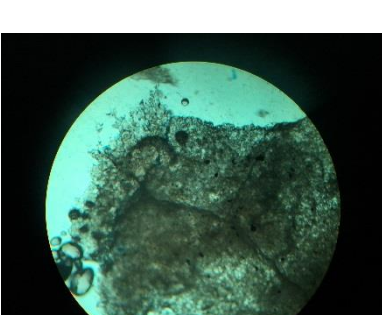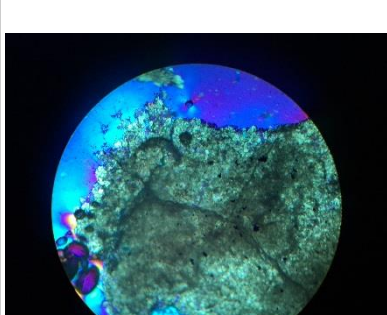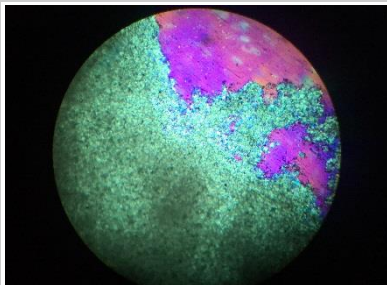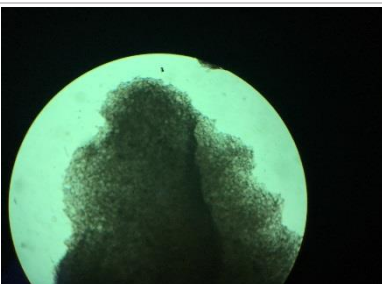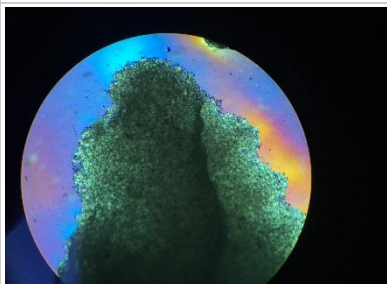
API	Depth (ft)	Porosity Type	Comments
19004	3260-3265	Intercrystalline, fracture	planer-e, coarsely crystalline, euhedral to subhedral
19004	3265-3270	Intercrystalline, fracture	planer-e, coarsely crystalline, euhedral to subhedral, oil staining
19004	3260-3265 (1/3)	Intercrystalline, fracture	planer-e, very coarsely crystalline, euhedral to subhedral
19004	3260-3265 (2/3)	Intercrystalline, fracture	planer-e, coarsely crystalline, euhedral to subhedral, oil staining along fractures
19004	3270 (1/3)	Intercrystalline, fracture	planer-e, coarsely crystalline, euhedral to subhedral
19004	3270 (2/3)	Fracture	planer-e, coarsely crustalline, euhedral to subhedral, oil staining along fractures
19008	2670-2675	Fracture, Intercrystalline	planer-s, coarse crystalline, euhedral to subhedral, good porosity, oil staining, calcite present in some dolomite samples
19008	2675-2680	Fracture	planer-s, coarse crystalline, subhedral, good porosity, one piece of oolitic, oil staining present, small amounts of calcite present in some dolomite
19008	2680-2685	Fracture	coarse crystalline, euhedral to subhedral, oil staining
19008	2685-2690	fracture	planer-e, medium crystalline, euhedral,
19008	2690-2695	Fracture, Intercrystalline, moldic	planer-e, medium crystalline, euhedral oolitic, 4mm across oolites
19008	2691.25	Fracture	planar-e, fine crystalline, euhedral to subhedral
19008	2691.5	Fracture, Intercrystalline	planer-e, fine coarse crystalline, euhedral
19008	3225-3230	Intercrystalline, fracture	planer-e, medium coarse crystalline, euhedral
19008	3230-3235	Intercrystalline, fracture	planer-e, medium coarse crystalline, euhedralto subhedral
19008	3240-3245	Intercrystalline, fracture	planer-e, coarse crystalline, euhedral to subhedral
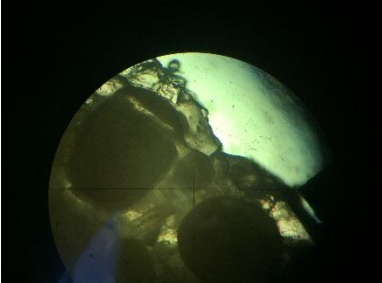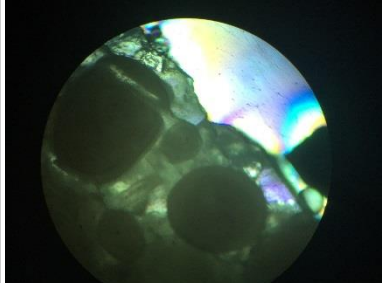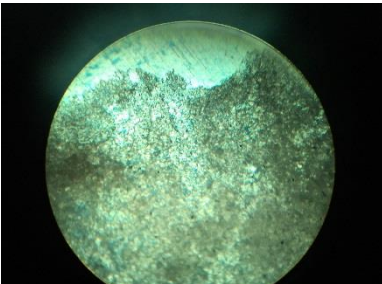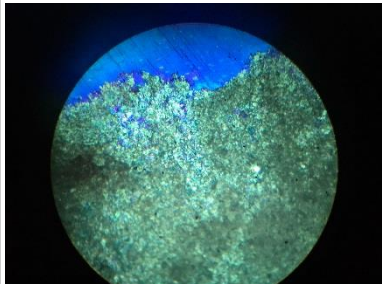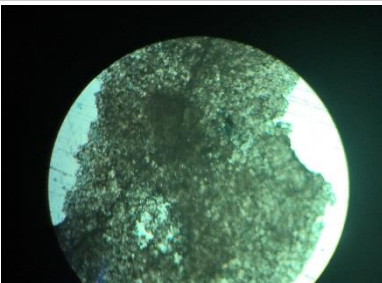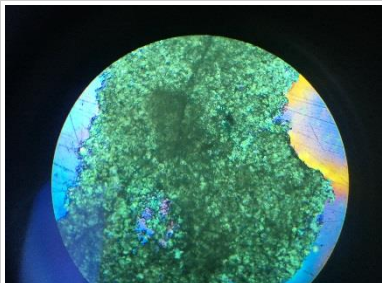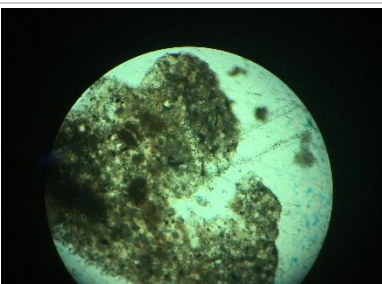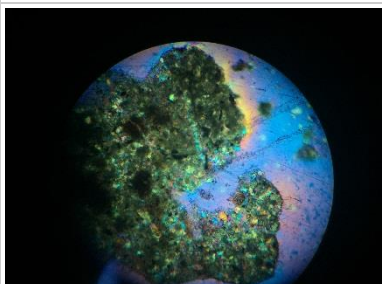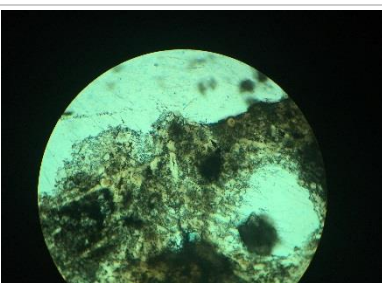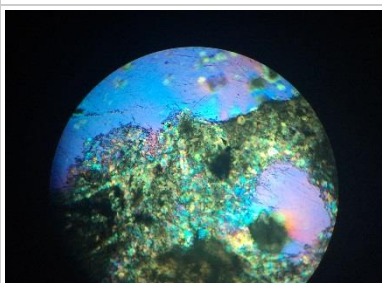
19008	3246.25	Intercrystalline, fracture	planer-s, medium crystalline, subhedral to anhedral, possible little fragments of chert
19008	3246.5	Fracture	planer-s, medium crystalline, subhedral to anhedral, possible little fragments of chert
19009	2720-2730	Fracture, Intercrystalline	planer-e, medium crystalline, euhedral to subhedral, lots of pyrite maybe alittle chert
19009	2730-2734	Fracture, Intercrystalline	planer-e, medium crystalline, euhedral to subhedral, less pyrite than previous
19009	2734-2740	Fracture, Intercrystalline	planer-e, medium crystalline, euhedral to subhedral, hardley any pyrite
19009	2740-2750	Fracture, Intercrystalline	planer-e, medium crystalline, euhedral to subhedral, no pyrite
19009	2750-2760	Fracture, Intercrystalline	planer-e, fine to medium crystalline, euhedral to subhedral, good show of porosity
19009	3270-3280	Fracture	planer-s, medium to coarse crystalline, euhedral to subhedral,
19009	3284 (1/2)	Fracture	planer-e, medium to coarse crystalline, euhedral to subhedral, possible ooilitic, large piece of calcite
19009	3284 (1hr)	Fracture	planer-e, medium to coarse crystalline, euhedral to subhedral
19010	3240-3250	Fracture, Intercrystalline	planer-e, medium crystalline, euhedral
19010	3253 (1/4)	Fracture, Intercrystalline	planer-e, medium crystalline, euhedral to subhedral
19010	3253 (1/2)	Fracture, Intercrystalline	planer-e, medium crystalline, euhedral to subhedral
19011	3290-3299	fracture	planer-s, very coarsley crystalline, subhedral, oil staining in fractures
19011	3299 (1/4)	fracture , Intercrystalline	planer-s, coarsley crystalline, oil stanined micrite, subhedral, oil staining in fratures
19011	3299 (1hr)	fracture, Intercrystalline, moldic	planer-e, very coarsely crystalline to coarsely crystalline, euhedral to subhedral, partial trilobite
19012	2707 (1/4)	Fracture	planer-s, fine to medium crystalline, subhedral to anhedral, large amounts of pyrite, some limestone
19012	2707 (1/2)	Fracture	planer-s, fine to medium crystalline, subhedral to anhedral, large amounts of pyrite, large piece of pyrite
19012	2707 (3/4)	Fracture, Intercrystalline	planer-e, fine to medium crystalline, hedral to subhedral, very large piece of pyrite
19033	2680-2690	Fracture	planer-e, very coarsely crystalline, euhedral, oil staining, large piece of pyrite
19033	2690-2700	Fracture	planer-s, subhedral, medium crystalline
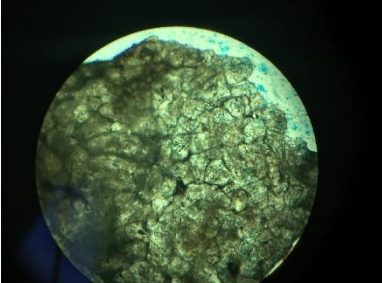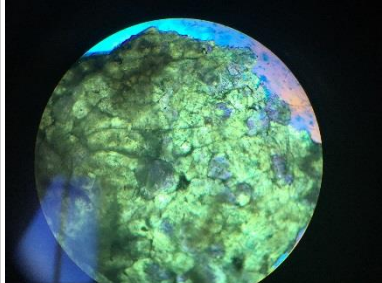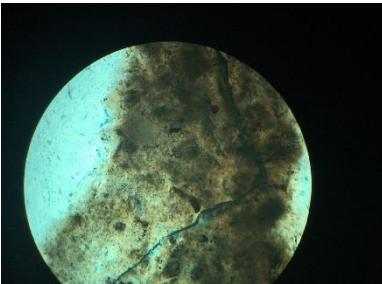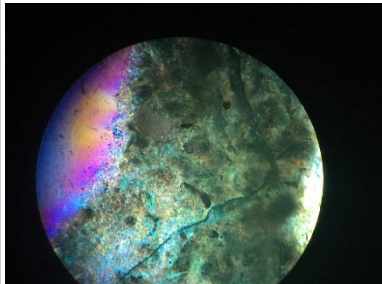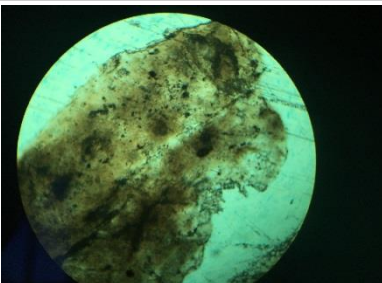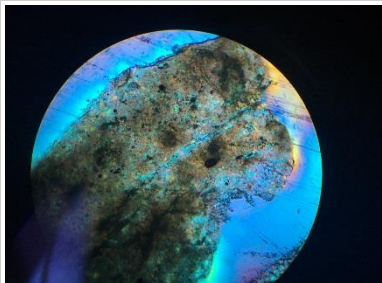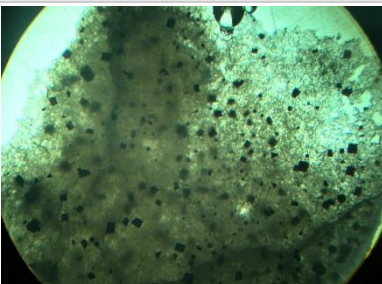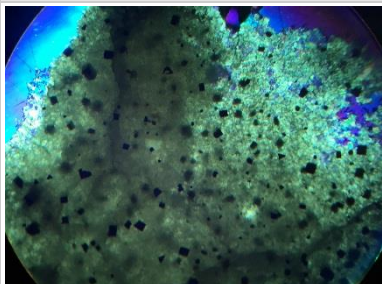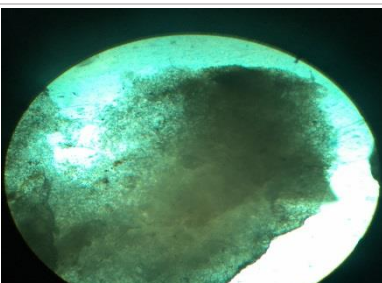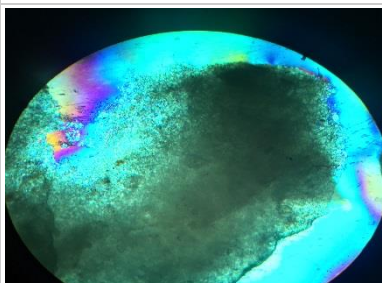
19033	2700-2710	Fracture	planer-s, subhedral, medium crystalline, possible piece of chert
19033	2710-2720	Fracture	planer-s, subhedral, medium crystalline
20032	2706 (5min)	Fracture	planer-s, coarsely crystalline, subhedral to anhedral, possible sponges filled with dolomite or calcite
20032	2706 (10min)	Fracture	planer-s, very fine crystalline, subhedral to anhedral possible calcite on edges, small piece of pyrite
20032	2707 (15min)	Fracture, Intercrystalline, moldic	planer-s, medium crystalline, subhedral to anhedral, oolitic, calcite present, possible sponge
20032	2710-2720	Fracture	planer-s, coarse crystalline, subhedral to anhedral, good prososity
20032	2717	Fracture	planer-s, very coarse crystallline, subhedral to anhedral, equaint crystals present
20032	3240-3250	Fracture	planer-s, coarse crystalline, euhedral to subhedral
20032	3250-3260	Fracture	planer-s, very coarse crystallline, subhedral, oil staining on fractures
20032	3260-3270	Fracture	planer-s, very coarse crystalline, hedral to subhedral, possible chert on edges
20032	3260 (20min)	Fracture	planer-s, very coarse crystalline, hedral to subhedral
20032	3260 (40min)	Fracture	planer-s, very coarse crystalline, hedral to subhedral
20032	3270-3280	Fracture	planer-s, subhedral, very coararse to coarse crystalline, good porisity showing
20032	3280-3290	Fracture	planer-s, subhedral to anhedral, very coararse to coarse crystalline, very fractured
20032	3290-3300	Fracture, Intercrystalline	planer-s, subhedral, very coarse crystalline, increasing crystal size down formation
20034	2670-2680	Fracture	planer-s, euhedral, finely crystalline, -- limestone present is very coarse crystalline
20034	2680-2690	Fracture, Intercrystalline	planer-s, euhedral to subuhedral, finely crystalline, small pieces of pyrite present
20034	2690-2700	Fracture, Intercrystalline	planer-s, euhedral to subuhedral, finely crystalline,
20034	3200-3210	Fracture, Intercrystalline	planer-s, euhedral to subuhedral, finely crystalline,
20034	3210-3220	Fracture	planer-s, subhedral, finely crystalline, oil staining present
20034	3220-3230	Fracture,	planer-e, subhedral to anhedral, finely crystalline, good porosity
20034	3230-3240	Fracture	planer-s, euhedral to subhedral, finely crystalline
20034	3240-50	Fracture	planer-s, euhedral to subhedral, finely crystalline
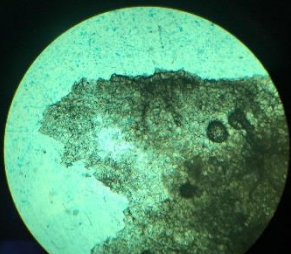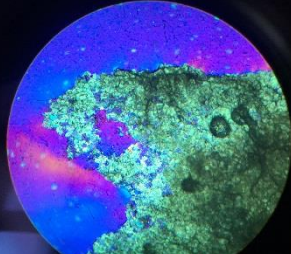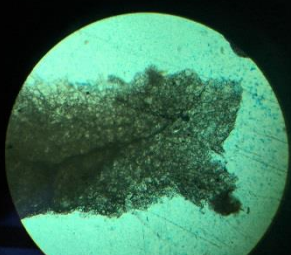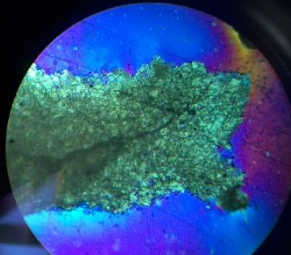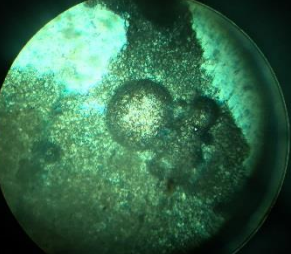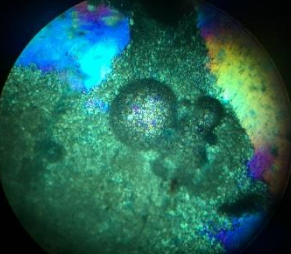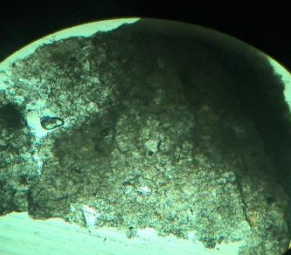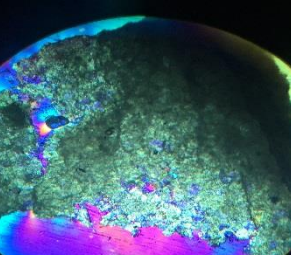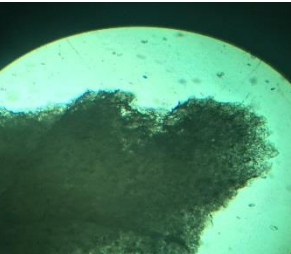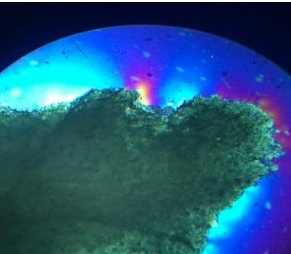
Table 2 - Petrographic Images at 10x magnification; Plain Polarized Light (PPL) and Cross Polarized Light (CPL).
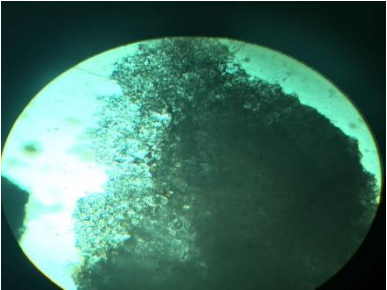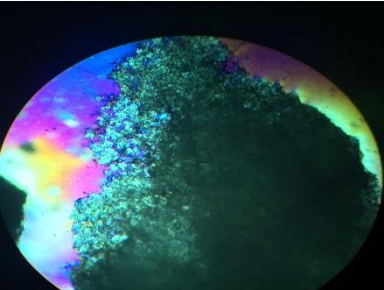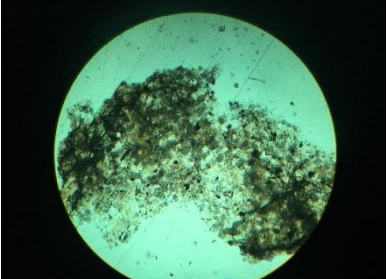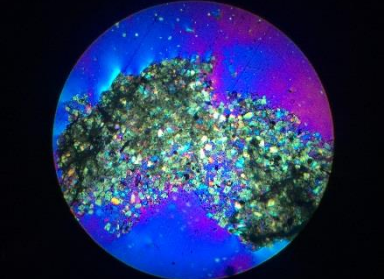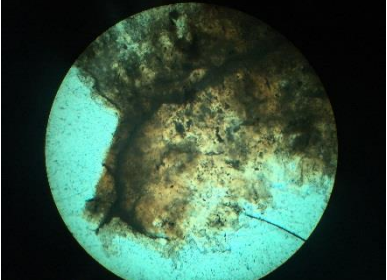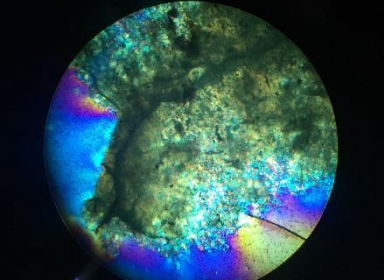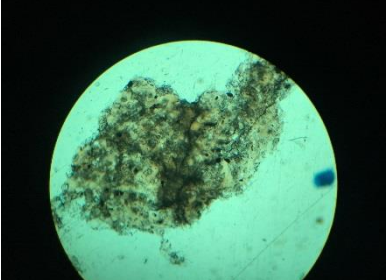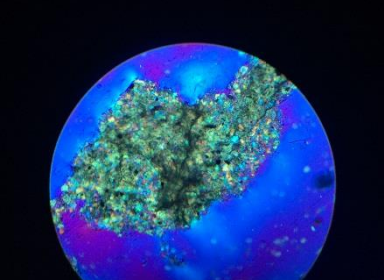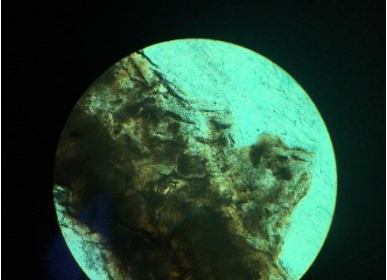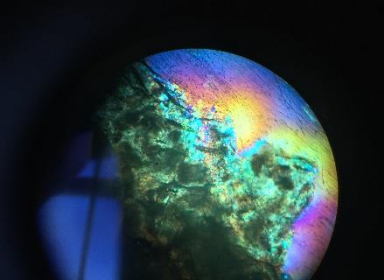
API	Depth (ft)	PPL	CPL
19004	3260-3265		
19004	3265-3270		
19004	3260-3265 (1/3)		
19004	3260-3265 (2/3)		
19004	3270 (1/3)		
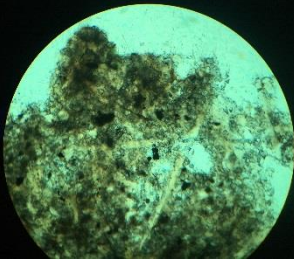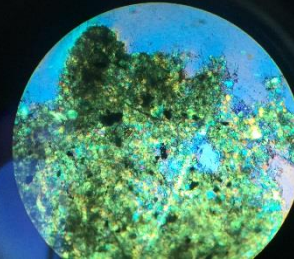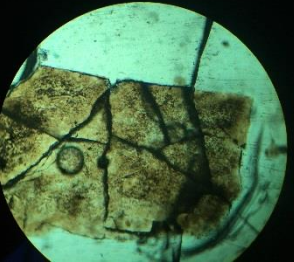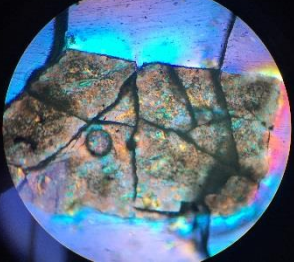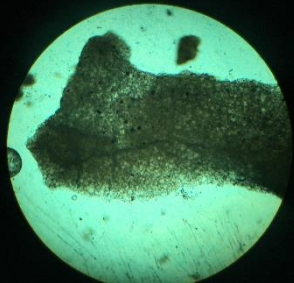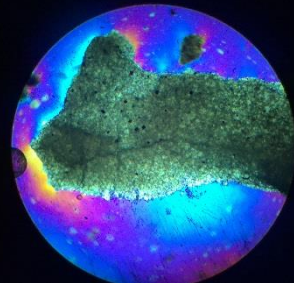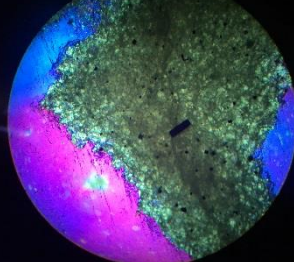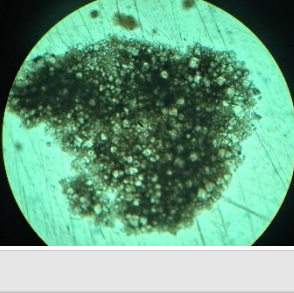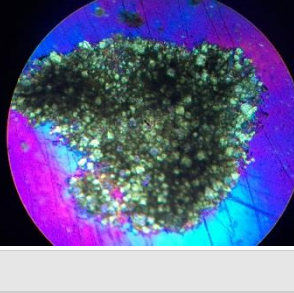
19004	3270 (2/3)		
19008	2670-2675		
19008	2675-2680		
19008	2680-2685		
19008	2685-2690		
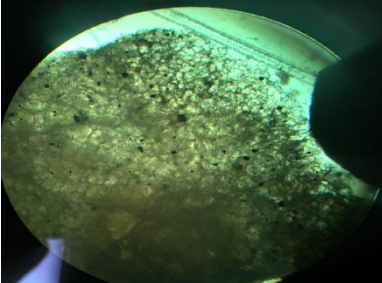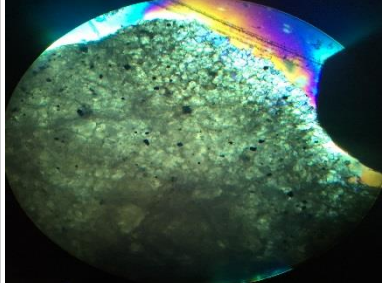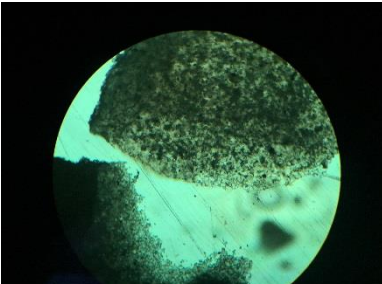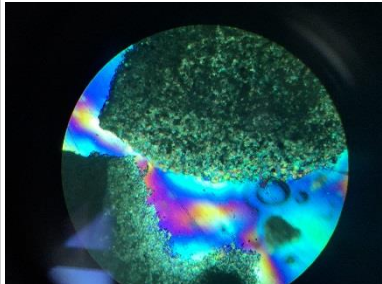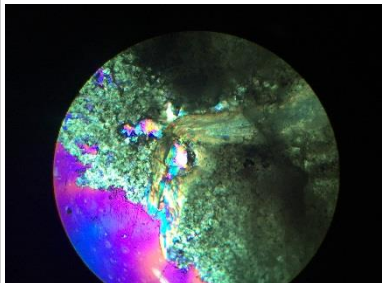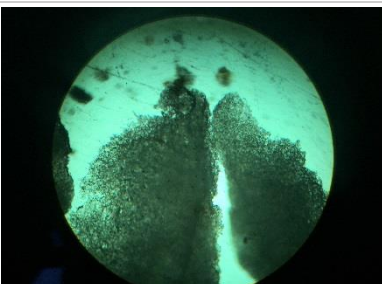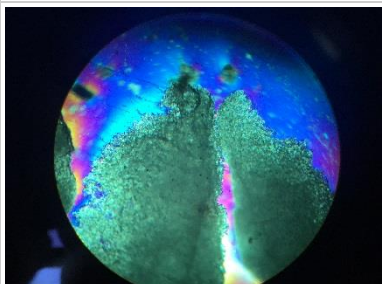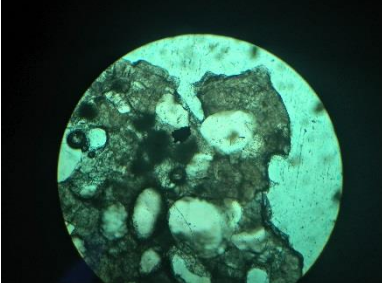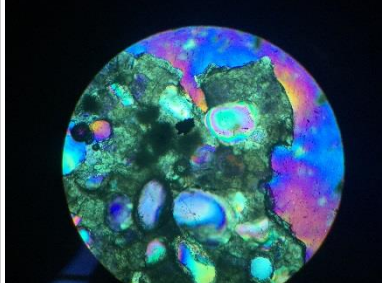
19008	2690-2695		
19008	2691.25		
19008	2691.5		
19008	3225-3230		
19008	3230-3235		
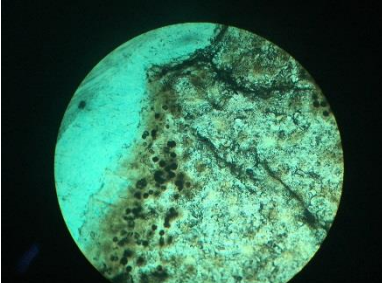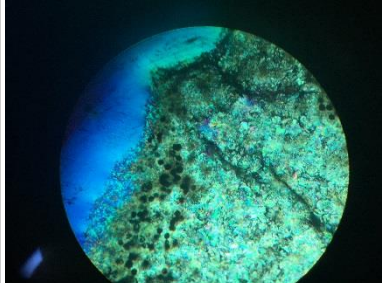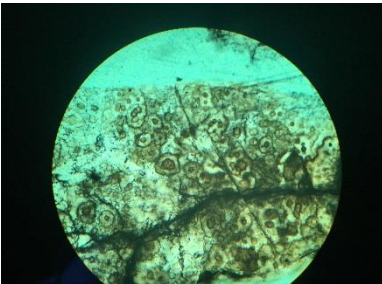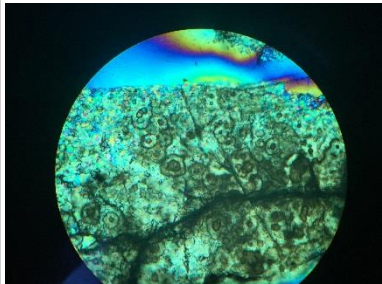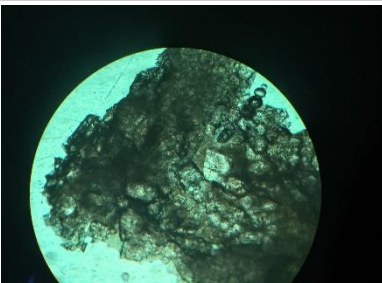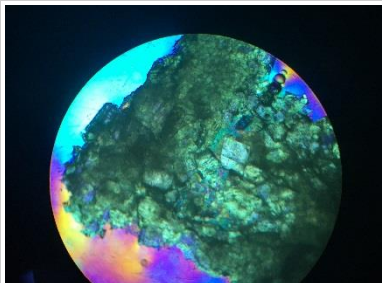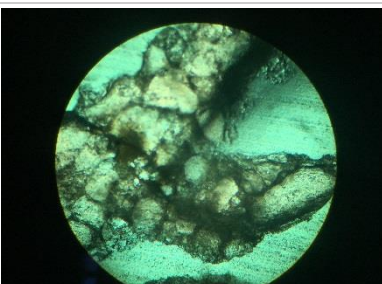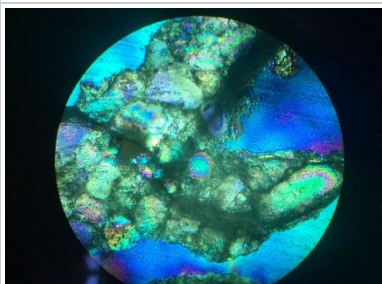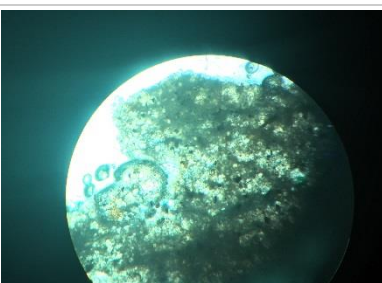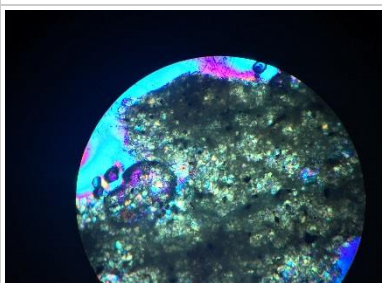
19008	3240-3245		
19008	3246.25		
19008	3246.5		
19009	2720-2730		
19009	2730-2734		
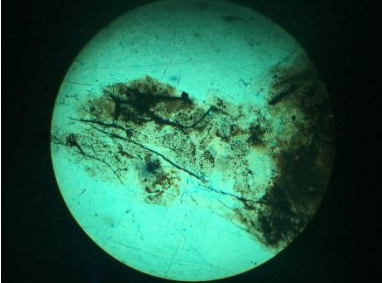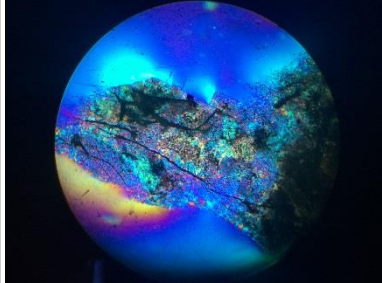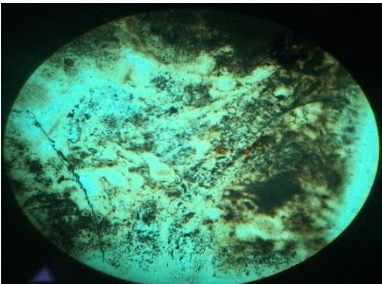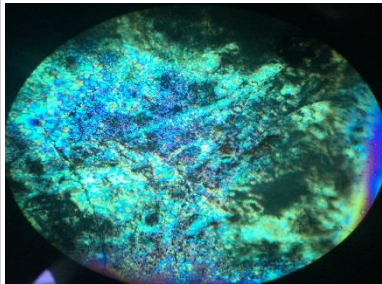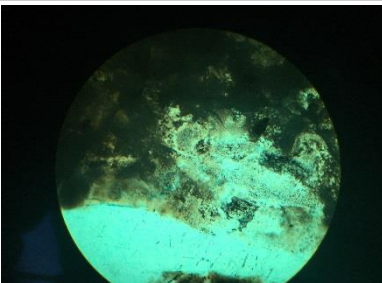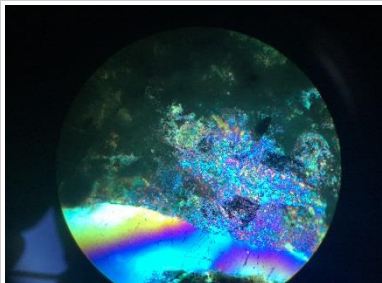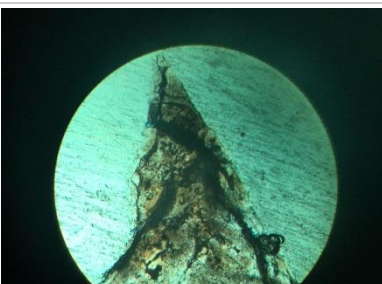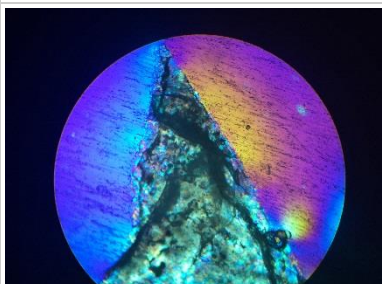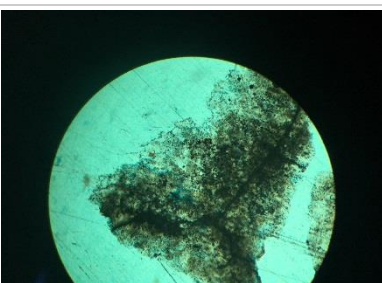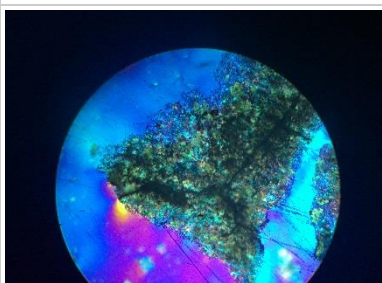
19009	2734-2740		
19009	2740-2750		
19009	2750-2760		
19009	3270-3280		
19009	3284 (1/2)		
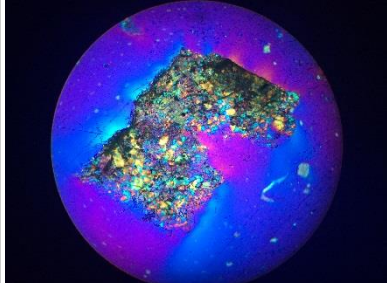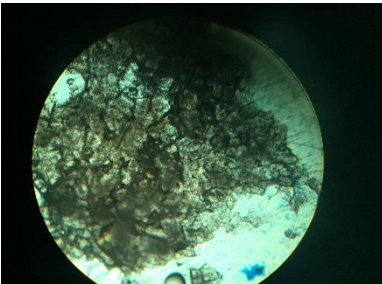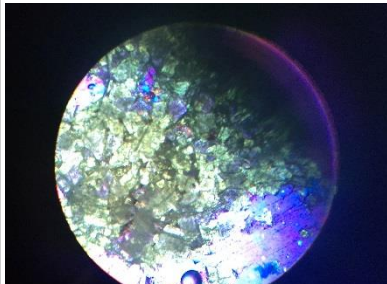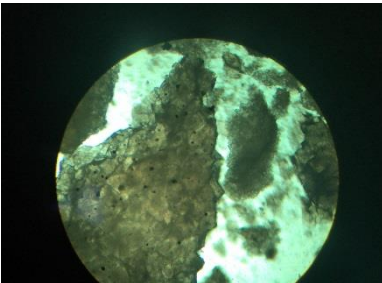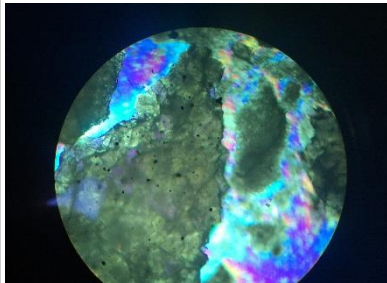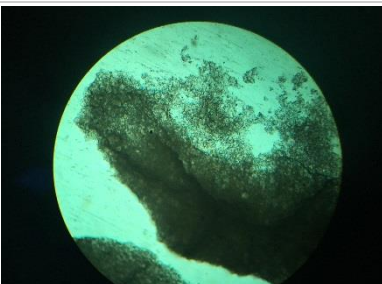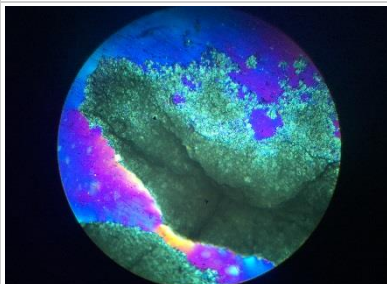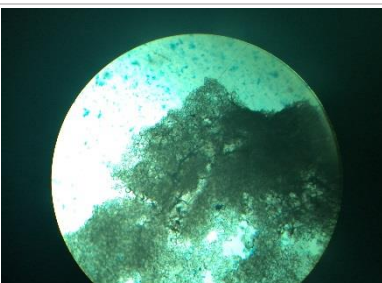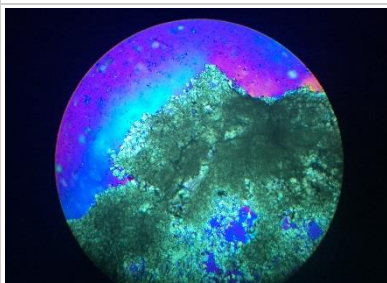
19009	3284 (1hr)		
19010	3240-3250		
19010	3253 (1/4)		
19010	3253 (1/2)		
19011	3290-3299		
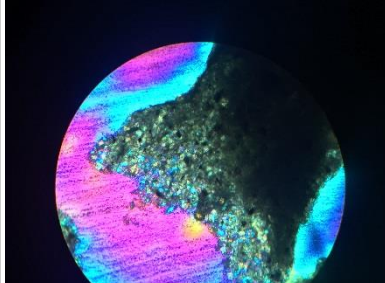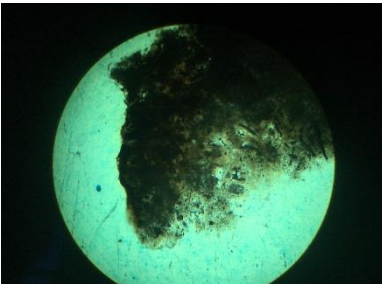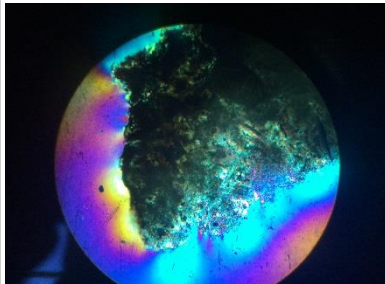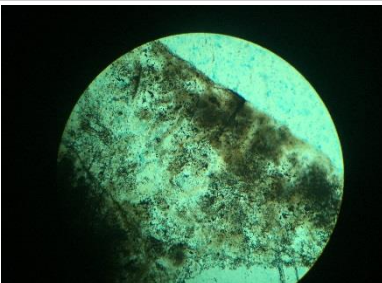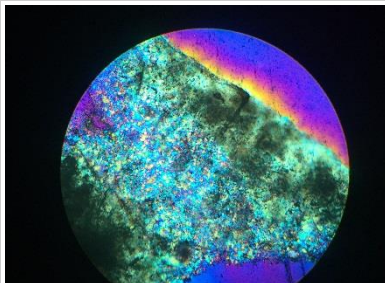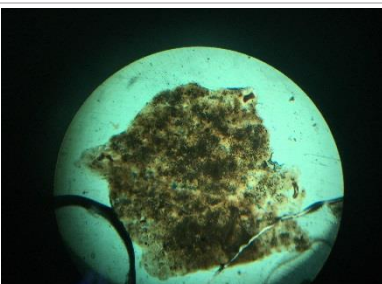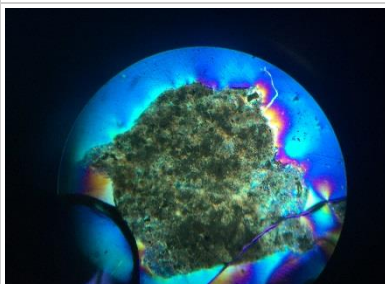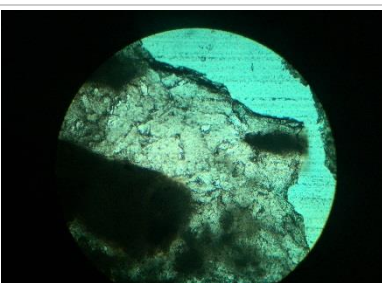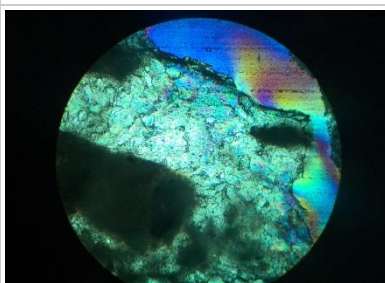
19011	3299 (1/4)		
19011	3299 (1hr)		
19012	2707 (1/4)		
19012	2707 (1/2)		
19012	2707 (3/4)		

19033	2680-2690		
19033	2690-2700		
19033	2700-2710		
19033	2710-2720		
20032	2706 (5min)		

20032	2706 (10min)		
20032	2706 (15min)		
20032	2710-2720		
20032	2717		
20032	3240-3250		

20032	3250-3260		
20032	3260-3270		
20032	3260 (20min)		
20032	3260 (40min)		
20032	3270-3280		

20032	3280-3290		
20032	3290-3300		
20034	2670-2680		
20034	2680-2690		
20034	2690-2700		

20034	3200-3210		
20034	3210-3220		
20034	3220-3230		
20034	3230-3240		
20034	3240-3250		
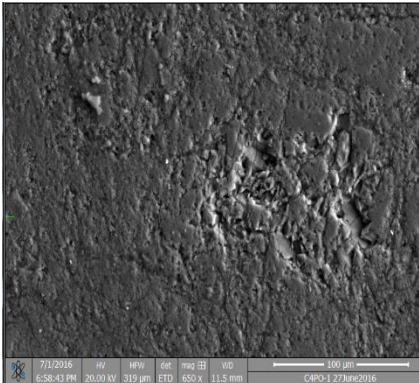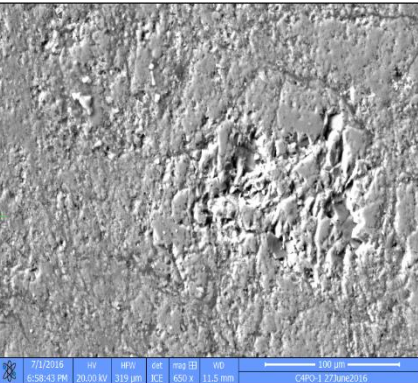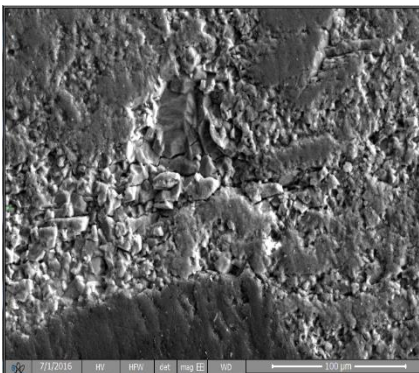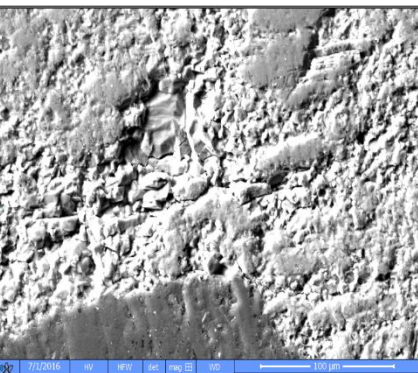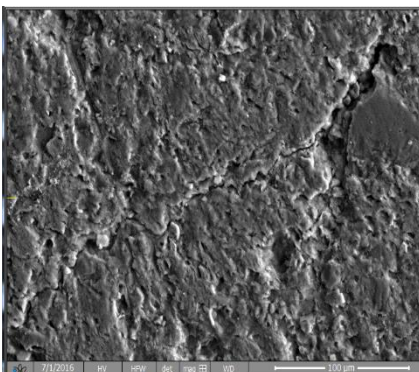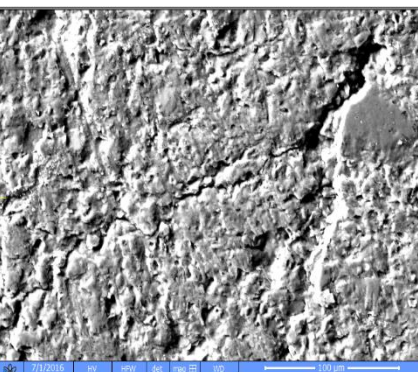
4.3 Dolomitization
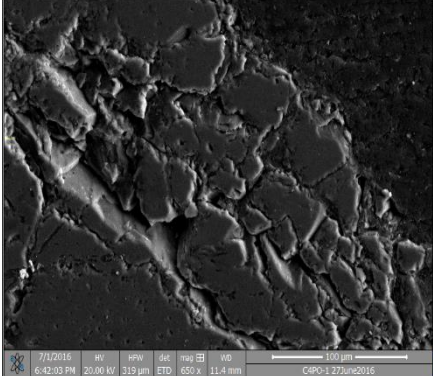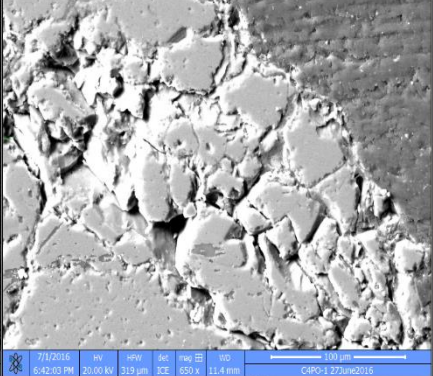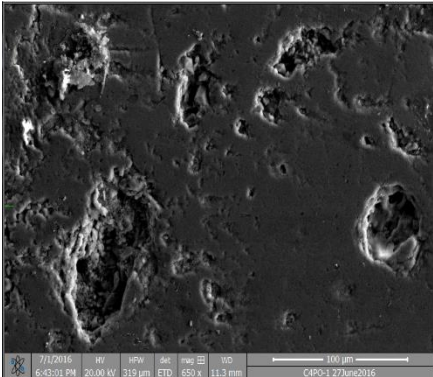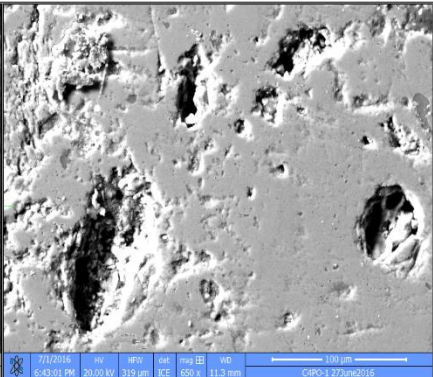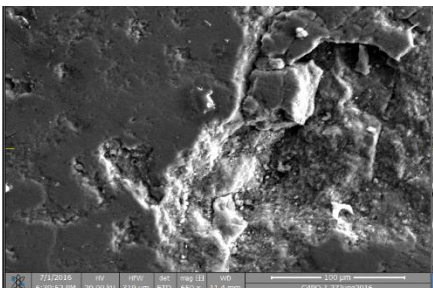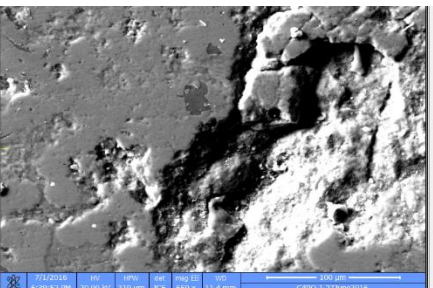
One of the benefits of examining well cuttings under petrographic microscope is that it shows the wide range of dolomite crystal size encountered through a formation, which could be a controlling factor in reservoir quality. Figure 13 displays a base map of the wells examined by thin section. Through petrographic analysis, and using the Scholle and Ulmer-Scholle's, (2003) classification, it was determined that dolomite crystal sizes ranged from 0.125mm (medium crystalline) to 3.5 mm (very coarsely crystalline). Crystal shape was also examined in the petrographic analysis, and samples displayed a large variety of shapes, including both planer types euhedral and subhedral. The upper section of both Hunton and Viola Limestones, where production is most prominent in this area appears to be composed of almost entirely dolomite. In the Hunton Formation it was not uncommon to see amounts of pyrite in samples along with very small amounts of chert and calcite. In the Viola Formation it was not uncommon to see little fragments of chert and some oolitic limestone features. Both formations had samples that had oil staining present.

4.4 Scanning Electron Microscope Results

Table 3 shows the results of selected drill cuttings examination under a scanning electron microscope. Two specific wells of interest were further examined and images were taken at 650 times magnification to better understand the porosity present. Two images were taken of each location, the first was a standard image (EDT) and the second was a higher performance secondary image (ICE).

Table 3 - Scanning Electron Microscope Results
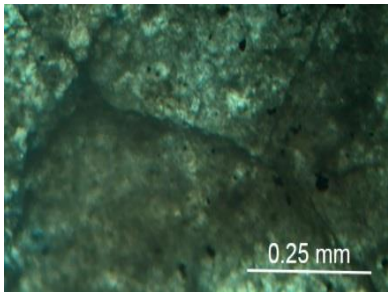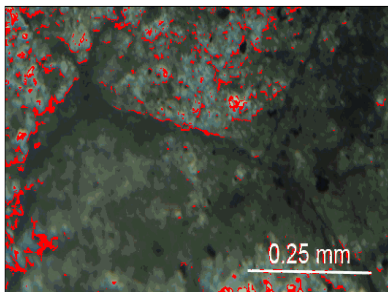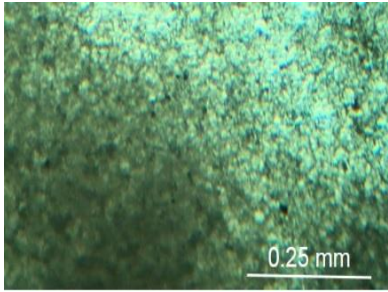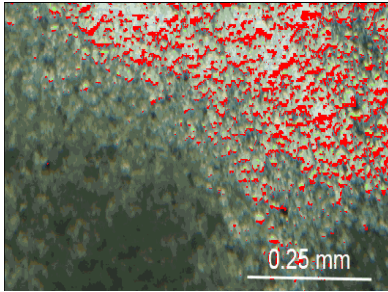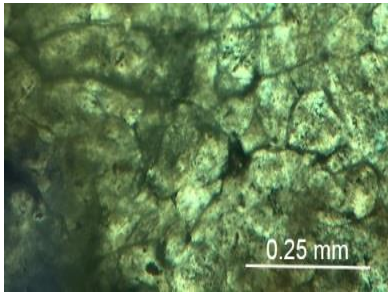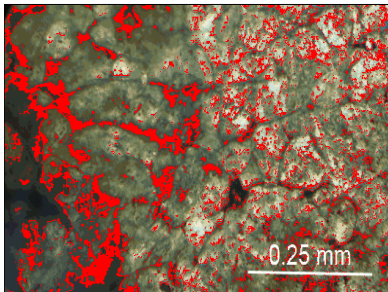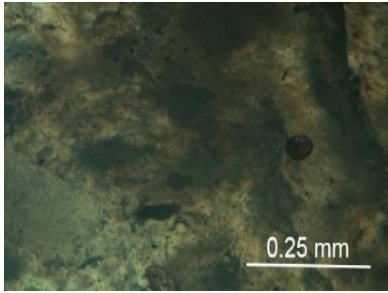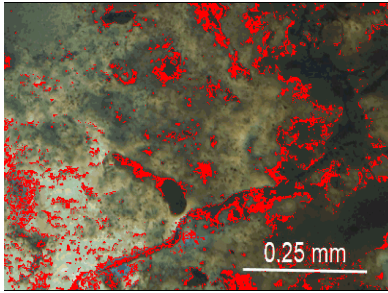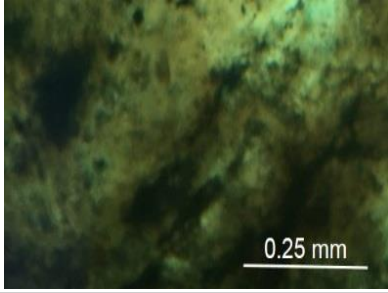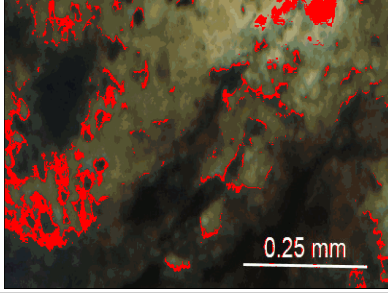
API	Depth (ft)	Scanning Electron Microscope Images
19011	3299 (20min)	
19011	3299 (20min)	
19011	3299 (20min)	
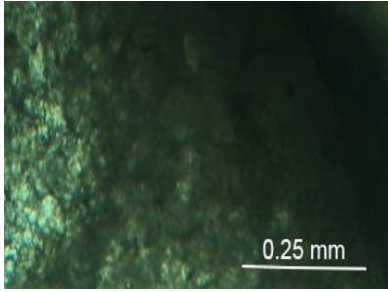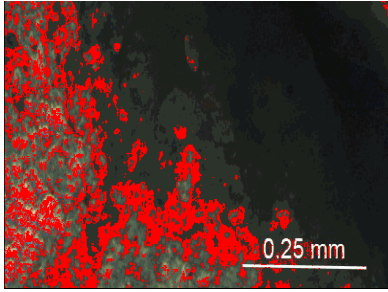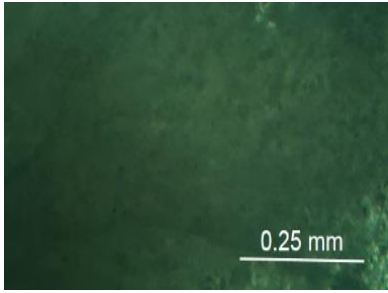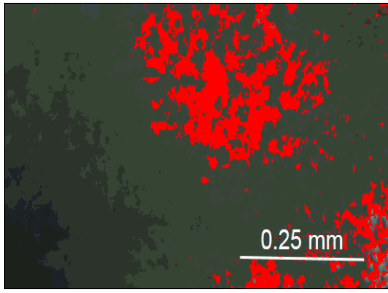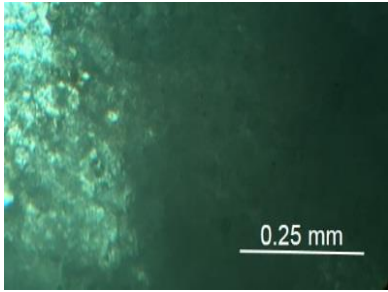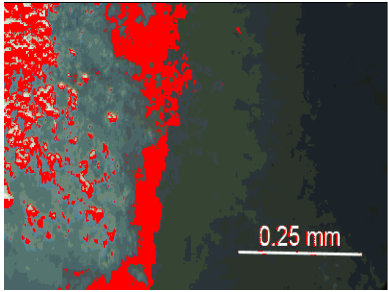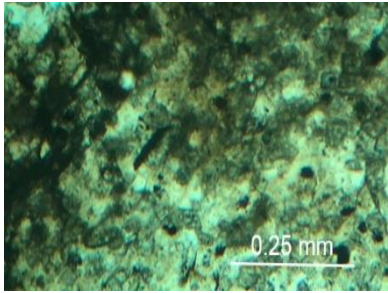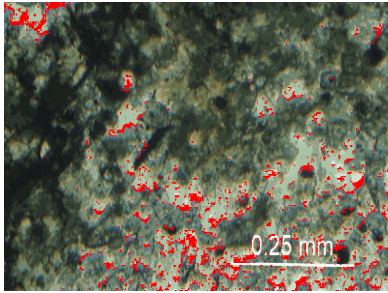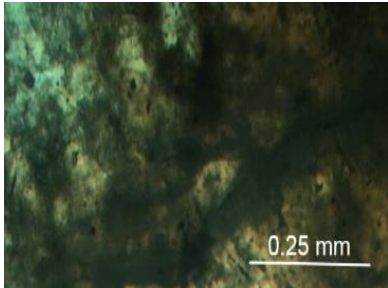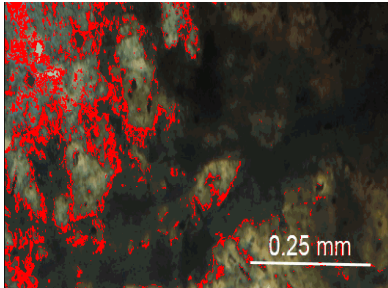
20032	3260 (20min)		
20032	3260 (20min)		
20032	3260 (20min)		
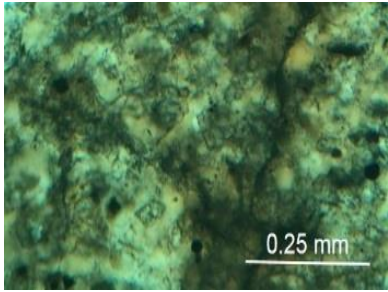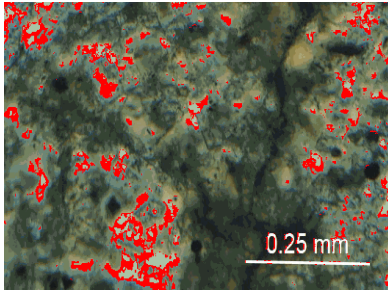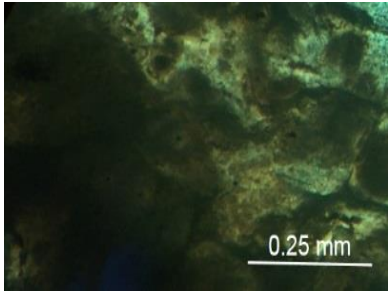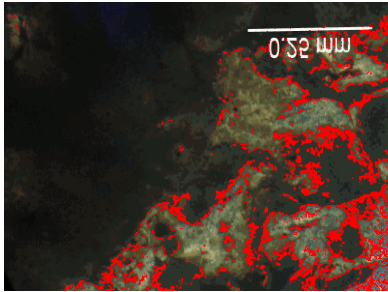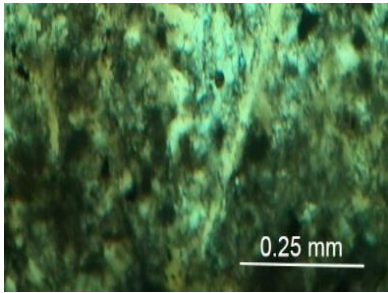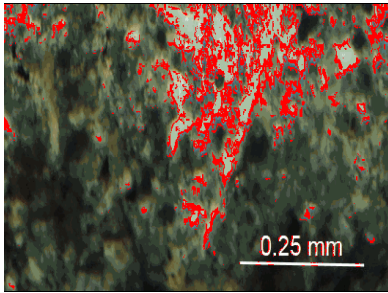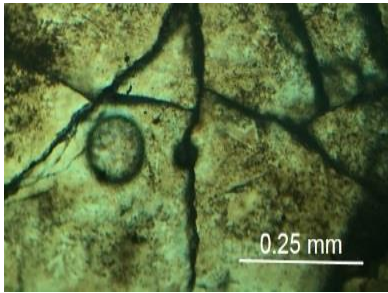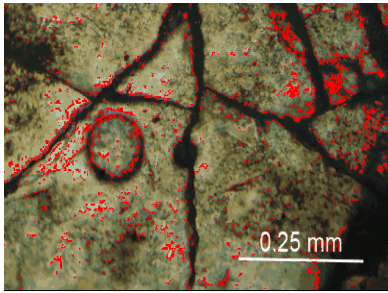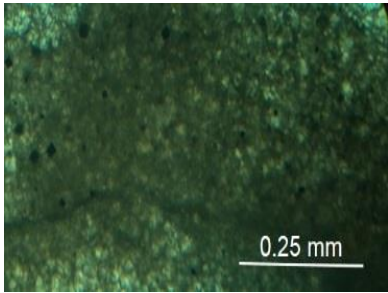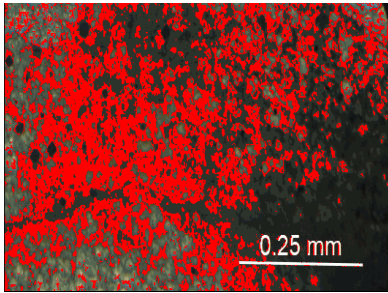
4.5 ImageJ Analysis Results
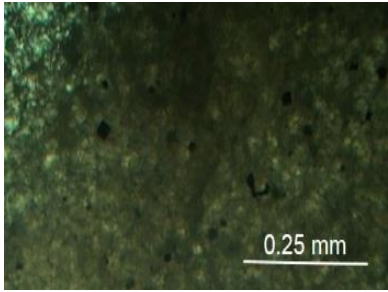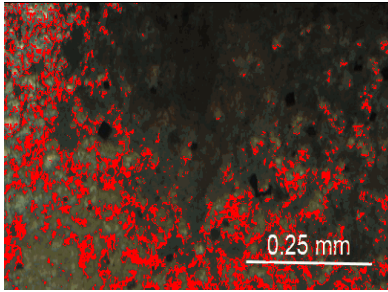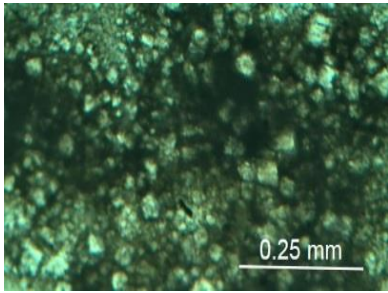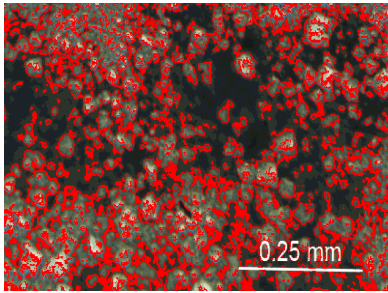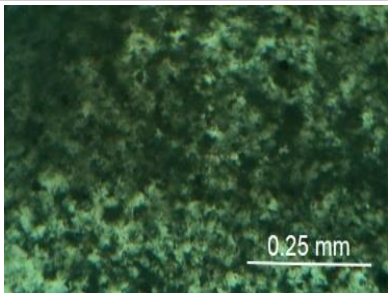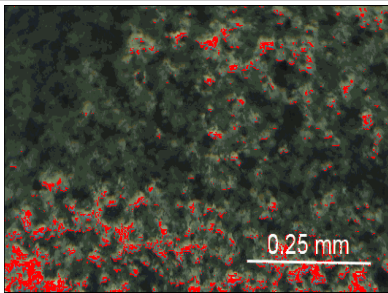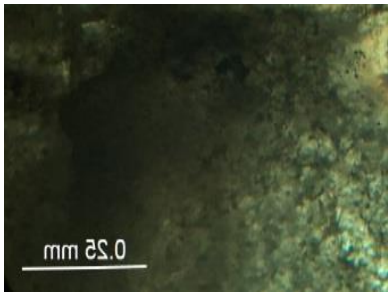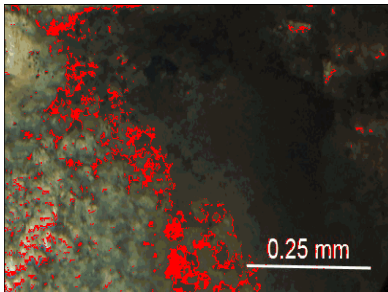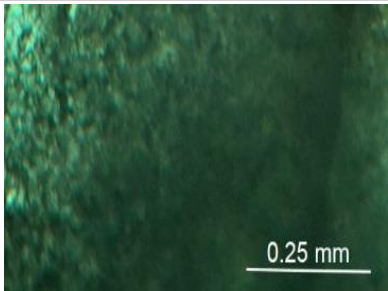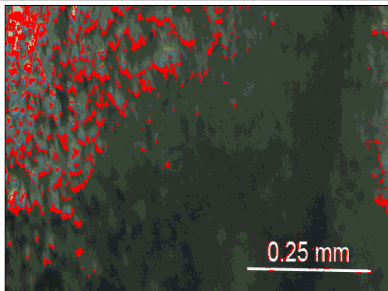
Table 4 shows photomicrographs that were taken during the petrographic analysis. The third column shows the images in plain polarized light and the fourth is the result of the ImageJ software manipulation. All images were taken with 10x magnification and a scale bar has been added. The last column of the table shows the porosity calculations for each image with the average well porosity being found in the blue highlighted row.
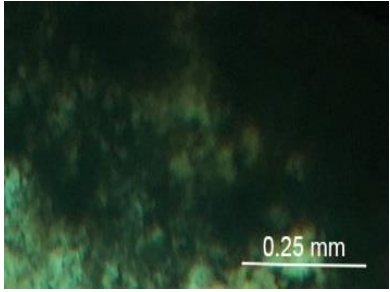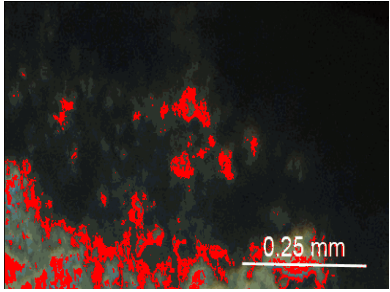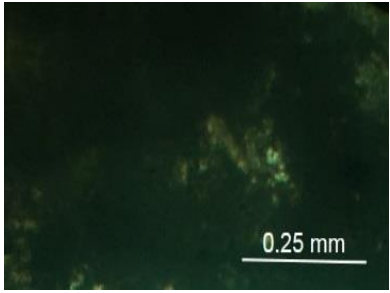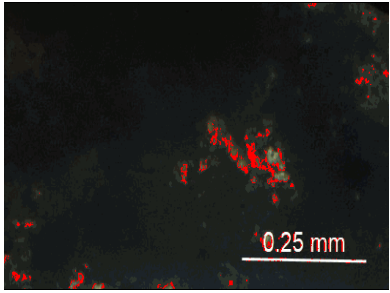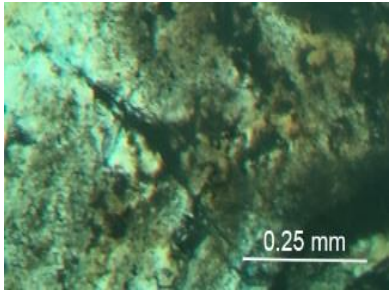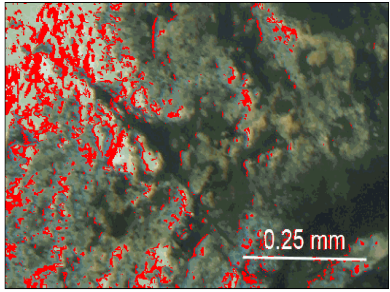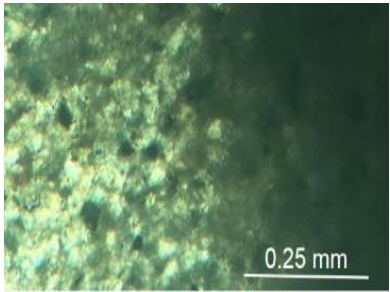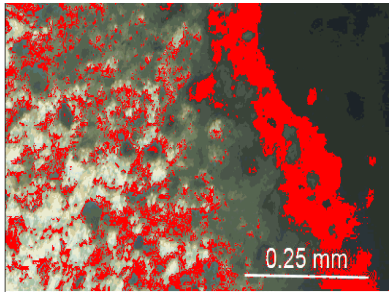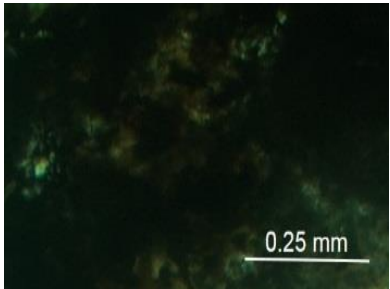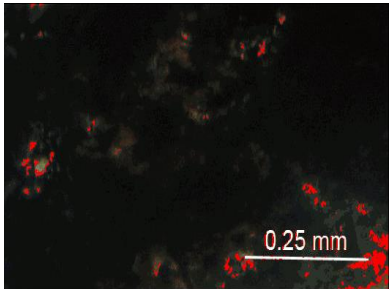
Table 4 - ImageJ Analysis Results

API	Depth (ft)	Photomicrograph at 10x	ImageJ Result (porosity shown in red)	Porosity Calculation
19004	3270 (1/3)			Total pixels= 157500 Pixels forming porosity= 6842 Porosity= 4.3441
19004	3270 (2/3)			Total pixels= 158025 Pixels forming porosity= 14505 Porosity= 9.1789
Average Porosity				**6.7615**
19008	3240-3245			Total pixels= 156975 Pixels forming porosity= 26233 Porosity= 16.7116
19008	3246.25			Total pixels= 156975 Pixels forming porosity= 17459 Porosity= 11.1222
19008	3246.5			Total pixels= 157500 Pixels forming porosity= 12442 Porosity= 7.8997
Average Porosity				**11.9111**

19009	3270-3280			Total pixels= 157500 Pixels forming porosity= 25567 Porosity= 16.233
19009	3284 (1/2)			Total pixels= 157500 Pixels forming porosity= 22290 Porosity= 14.1524
19009	3284 (1hr)			Total pixels= 157500 Pixels forming porosity= 22471 Porosity= 14.2673
Average Porosity				**14.8842**
19010	3240-3250			Total pixels= 156975 Pixels forming porosity= 7600 Porosity= 4.8415
19010	3253 (1/4)			Total pixels= 157500 Pixels forming porosity= 15664 Porosity= 9.9454

19010	3253 (1/2)			Total pixels= 157500 Pixels forming porosity= 11044 Porosity= 7.0121
Average Porosity				**7.2663**
19011	3290-3299			Total pixels= 156975 Pixels forming porosity= 13811 Porosity= 8.7982
19011	3299 (1/4)			Total pixels= 157500 Pixels forming porosity= 15603 Porosity= 9.9067
19011	3299 (1hr)			Total pixels= 157500 Pixels forming porosity= 10185 Porosity= 6.4667
Average Porosity				**8.3905**
19012	2707 (1/4)			Total pixels= 156975 Pixels forming porosity= 56343 Porosity= 35.893

19012	2707 (1/2)			Total pixels= 157500 Pixels forming porosity= 22132 Porosity= 14.0521
19012	2707 (3/4)			Total pixels= 157500 Pixels forming porosity= 41798 Porosity= 26.5384
Average Porosity				**25.4945**
19033	2690-2700			Total pixels= 157500 Pixels forming porosity= 8053 Porosity= 5.113
19033	2700-2710			Total pixels= 157500 Pixels forming porosity= 9517 Porosity= 6.0425
19033	2710-2720			Total pixels= 157500 Pixels forming porosity= 10217 Porosity= 6.487
Average Porosity				**5.8808**

20032	3260-3270			Total pixels= 157500 Pixels forming porosity= 12688 Porosity= 8.0559
20032	3260 (20min)			Total pixels= 157500 Pixels forming porosity= 2050 Porosity= 1.3016
20032	3260 (40min)			Total pixels= 157500 Pixels forming porosity= 16336 Porosity= 10.3721
Average Porosity				**6.5765**
20034	3200-3210			Total pixels= 158025 Pixels forming porosity= 38174 Porosity= 24.1569
20034	3210-3220			Total pixels= 157500 Pixels forming porosity= 2328 Porosity= 1.4781
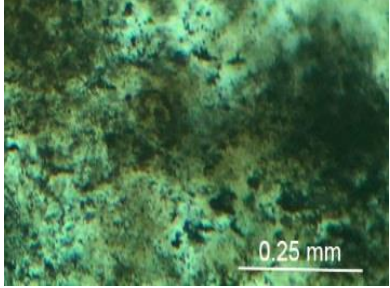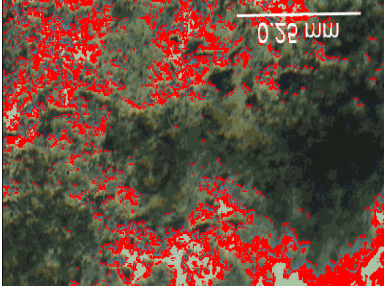
20034	3220-3230			Total pixels= 157500 Pixels forming porosity= 27806 Porosity= 17.6546
Average Porosity				**14.4298**

Table 5 - Table showing the well names, the sampled and studied interval, the calculated porosities for each interval using ImageJ.

API	Studied Depth (ft)	ImageJ Porosity
19004	3270 (1/3)	4.3 %
19004	3270 (2/3)	9.1 %
19008	3240-3245	16.7 %
19008	3246.25	11.1 %
19008	3246.5	7.9 %
19009	3270-3280	16.2 %
19009	3284 (1/2)	14.1 %
19009	3284 (1hr)	14.2 %
19010	3240-3250	4.8 %
19010	3253 (1/4)	9.9 %
19010	3253 (1/2)	7.0 %
19011	3290-3299	8.8 %
19011	3299 (1/4)	9.9 %
19011	3299 (1hr)	6.5 %
19012	2707 (1/4)	35.9 %
19012	2707 (1/2)	14.1 %
19012	2707 (3/4)	26.5 %
19033	2690-2700	5.1 %
19033	2700-2710	6. %
19033	2710-2720	6.5 %
20032	3260-3270	8.0 %
20032	3260 (20min)	1.3 %
20032	3260 (40min)	10.3 %
20034	3200-3210	24.1 %
20034	3210-3220	1.4 %
20034	3220-3230	17.6 %

Chapter 5 - Discussion

5.1 Structure and Production

A common petroleum trapping mechanism found in the Forest City Basin is an anticlinal structure with closure that trends in a northeast-southwest direction, and the Leach Field is no different. Oil production in the Leach Field roughly correlates to the subsurface structure maps created using IHS Petra®. Subsurface maps created display the tops of the two formations of interest, the Hunton Limestone and Viola Limestone. In Figure 10, the Hunton Formation top shows that current production correlates closely to the structure of this formation. Figure 11 shows the top of the Viola Formation, and it also appears to generally correlate with the oil production being found near the structural high of the formation, with non-producers surrounding the flanks of the high. In both of these maps, however there are instances where wells that are down structure appear to be more productive than wells on structure. This suggests an additional control on production. To further examine this, I looked at two wells, the Hladkey A1 and the Hladkey 4. Figure 15 shows these wells highlighted on both the Hunton and Viola Limestone structure map. The Hladkey 4 is 47 feet up structure on the Hunton from the Hladkey A1, and 49 feet up structure on the Viola Formation. The initial production of the Hladkey 4 (up structure) was 15 barrels of oil and 200 barrels of water a day, compared to the Hladkey A1 (down structure) which initially produced 60 barrels of oil and 100 barrels of water a day. It appears that to some extent in the Leach Field structure does determine where oil can be encountered. However, some wells located in less favorable structure position have out produced wells up structure, suggesting that the difference in production must be a function of reservoir quality.

Figure 15 - Structure maps of the Hunton and Viola Limestones highlighting the structure difference in the Hladkey 4 and Hladkey A1.
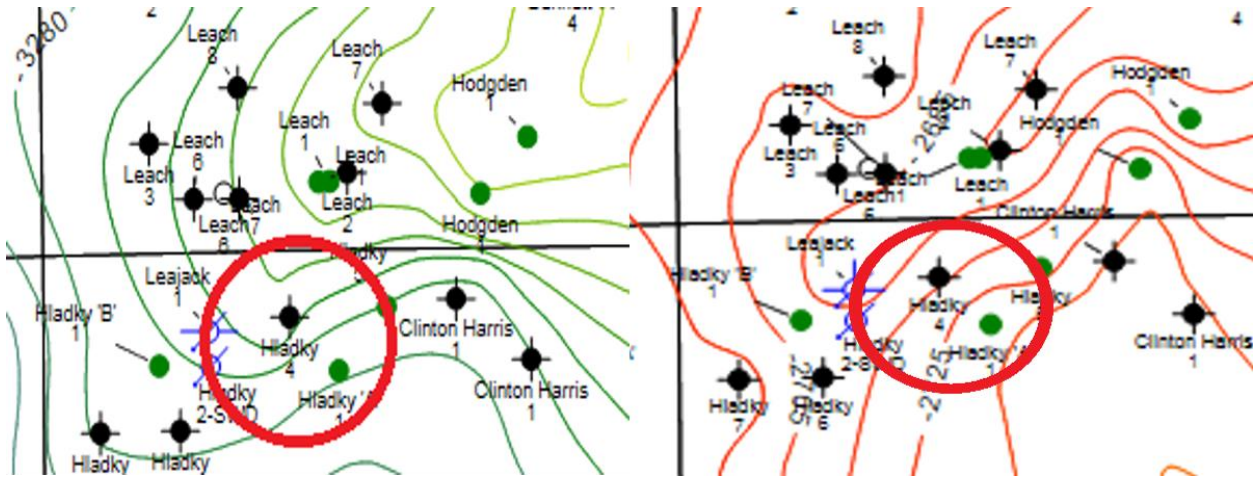
Figure 16 - Comparison of petrographic results for Hladkey 4 (left) and Hladkey A1 (right).
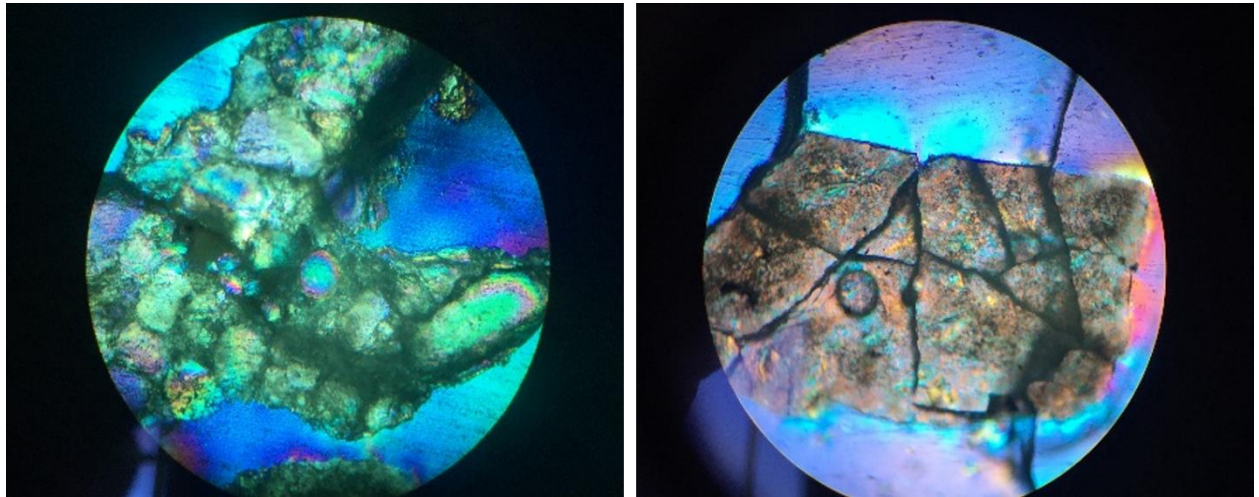
Looking more closely at the two wells examined earlier, Hladkey 4 and Hladkey A1 there appears to be a significant difference in petrographic analysis results (Figure 16). The Hladkey 4 well, in a structural high, showed very coarsely crystalline, subhedral (planer-s) crystals, with increasing crystal size down the formation. The Hladkey A1 well, in a structural low, showed euhedral (planer-e) crystals with very coarsely crystalline, and significant oil staining.

Scanning electron microscope analysis allowed for an even closer look at the features found during the petrographic analysis. SEM images were taken of one thin section for each well at a similar depth, these images were taken at 650 times magnification. Figure #17 compares these image results for the two wells. The Hladkey A1 (top) shows much more porosity and granular texture due to dolomitzation compared the Hladkey 4 (bottom) which appears smoother and less altered.

The use of the ImageJ software allowed for the estimate of porosity of the wells both in the structural high and those off structure. The results of testing further showed that it is not structure that is completely controlling production in the Leach Field, but rather reservoir quality. Further comparing of the Hladkey 4 (up structure) and Hladkey A1 (down structure) based on the average porosity percentages (Table 4) of the rocks found through the Image J process supports this idea. In the results the Hladkey 4 had an average porosity percentage of 6.5%, compared to an average of 8.4% for the Hladkey A1. Figure 18 displays samples of results from the ImageJ porosity calculation process, where on the left the Hladkey 4 calculated a porosity of 1.3% and the Hladkey A1 calculated a porosity of 9.9%. These results show that even though the Hladkey A1 was down structure it had better porosity, which may explain its proven better hydrocarbon production.

Figure 17 -Scanning Electron Microscope results for Hladkey A1 (top) and Hladkey 4 (bottom). The left image is a standard image (EDT) and the right image is a higher performance secondary image (ICE).
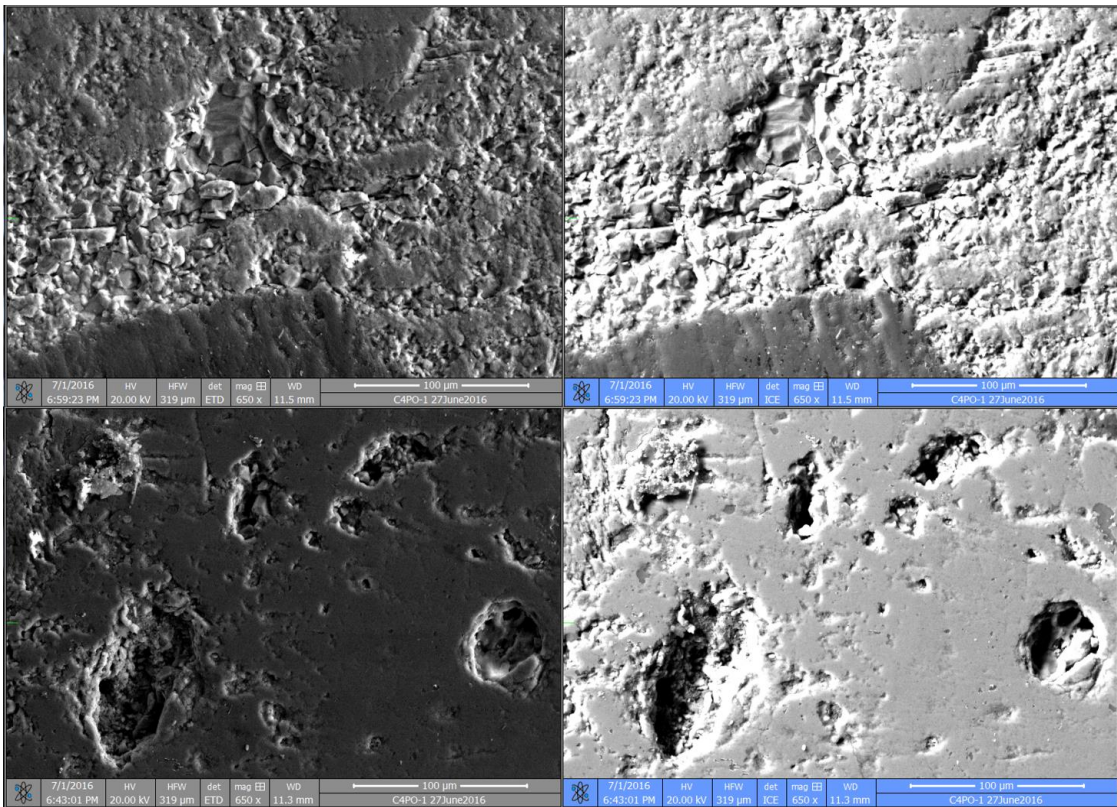
Figure 18 – Comparison of ImageJ porosity calculation results for the Hladkey 4 (left) and Hladkey A1 (right).
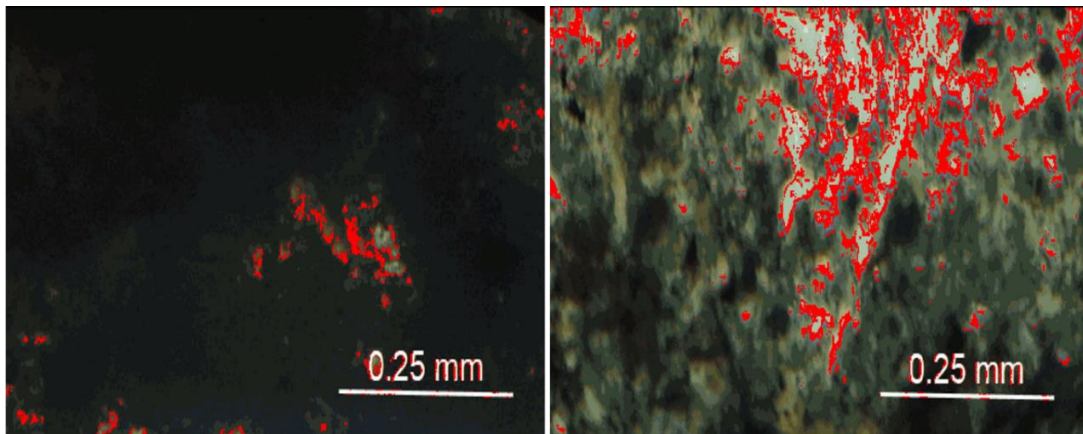
Hladkey 4 – 3260ft 20min

Total pixels= 157500
Pixels forming porosity= 2050
Porosity= **1.3016**

Hladkey "A"1 – 3299ft 15 min

Total pixels= 157500
Pixels forming porosity= 15603
Porosity= **9.9067**

Another example found where a well up structure being less productive than a well down structure is the Leach A2 and the Leach 8, (Figure 19). Both wells were completed into the Hunton Formation. The Leach A2 was drilled in 1964 and initially produced 78 barrels of oil per day. The Leach 8 was drilled in 1987 as part of the effort to infield drill the field, and it initially produced 50 barrels of oil per day. According to available completion cards the Leach A2 encountered the Hunton formation at 2727 feet, whereas the Leach 8 encountered it at 2720 feet, making the Leach 8 up structure by 7 feet. Lack of well cuttings for the Leach 8 makes it impossible to further examine the rock properties in thin section.

Figure 19 – Location of Leach A2 and Leach 8 on structure map of the Hunton Limestone.
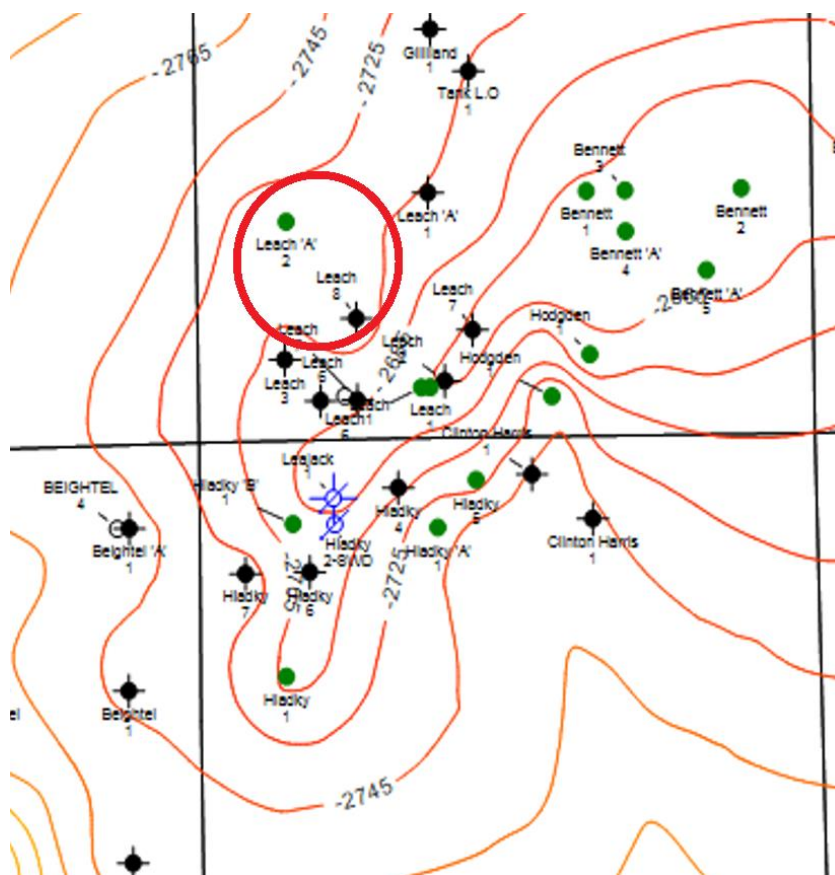
5.2 Reservoir Quality

Every well examined by thin section showed fracture porosity and a trend of increasing porosity with increasing crystal size. Due to the larger crystal size, the dolomite does not fit together as tightly, leaving more void space between the crystals thus resulting in an increased average porosity. Fractures are important in a reservoir because they connect pores, creating permeability that may not have been present originally. Also present in many samples was intercrystalline porosity which is beneficial because it means the porosity is well connected and can connect the many fractures or vugs present in the rock. In the result of average porosity percentages there appears to be no obvious correlation between porosity percentage and structure. Figure 20 show the very top of each formation outlined in a shape, Hunton (orange), and Viola (blue). There is pattern of evidence to prove that there is a drop off in porosity as wells move off structure, further proving that it is reservoir quality that is driving production and not structure.

Figure 20 – Average rock porosity results from Image J analysis. Outlined is the top of the producing formations, taken form the structure maps. Hunton Formation is shown in orange and the Viola Formation is shown in blue.
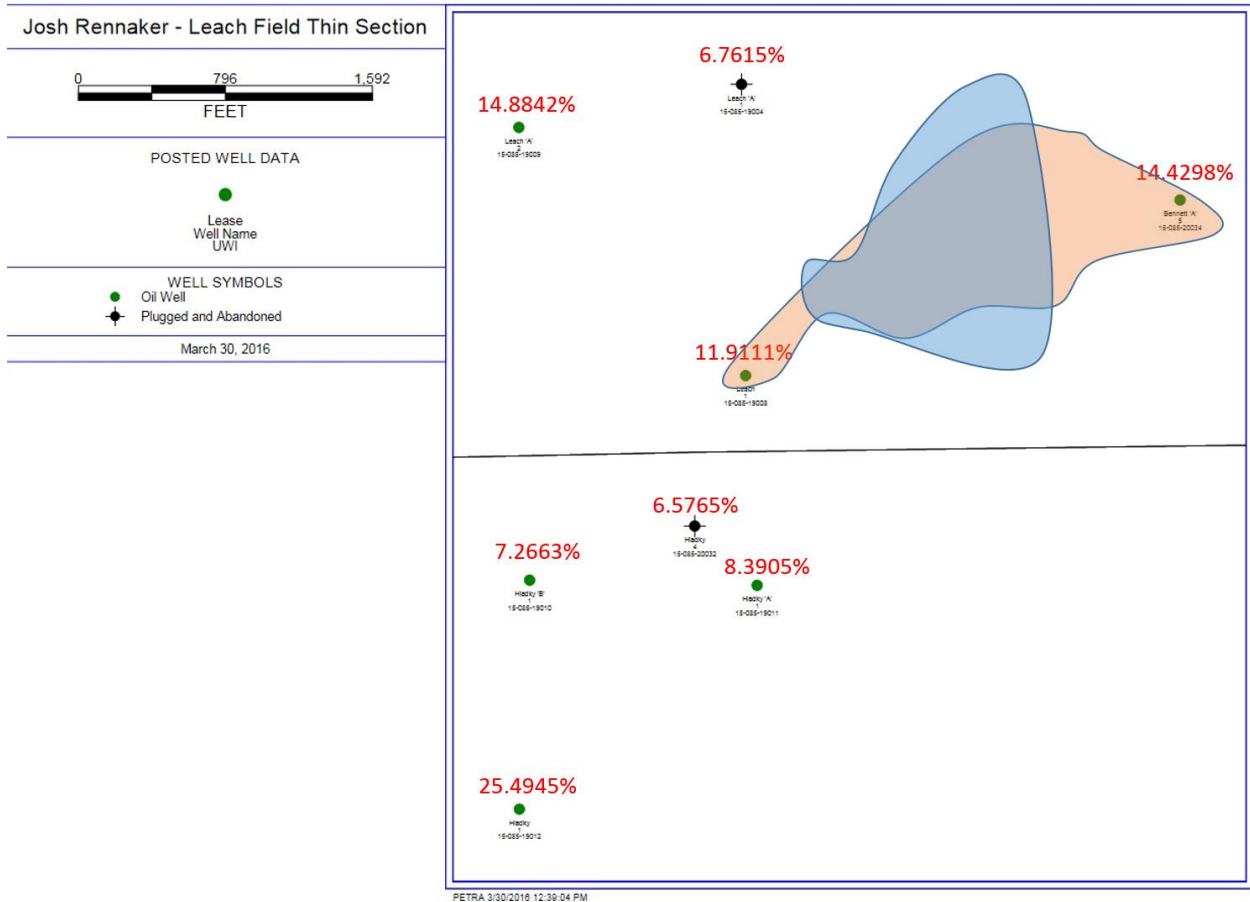
5.3 Understanding the Results

As previously mentioned the structure of the formations control where the reservoir will be found but does not explain how wells down structure have proved to be better and longer producing wells. The examination of drill cuttings under petrographic microscope gave the best insight to how the reservoir quality can control production. For the two wells highlighted in this study it is easy to see the differences in the size of the dolomite crystals and the degree of dolomitization, which directly affect the average porosity of the formation. These larger crystals sizes produce a better reservoir, because the overall porosity and permeably are higher than non-

dolomitized units. The reason for structure flanking wells out producing mid-structure well is believed to have been discovered by Lee (2005) in his research on the Forest City Basin. Based on microscope examination, Lee (2005) discovered that there was a correlation between samples that appeared to be a period of deformation of the rocks soon after their deposition. These deformations created local anticlinal highs in the Hunton and Viola Formations. As these formations were buried the basin continued to sink and these anticlinal highs gained in relief. It is believed that this caused these formations to undergo diagenesis and dolomite recrystallization several times (Lee, 2005). The result of this repeated recrystallization is different size dolomite crystal thorough each formation, thus leading to different average porosities. Lee also discovered that regional dip of the eastern side of the Forest City Basin has altered in direction over time. After deposition of the Ordovician system, regional dip of the area was reversed to the northwest. During the Nemaha uplift in the late Paleozoic age, that dip was reversed to a steeper southeast direction. Lee (2005) hypothesized that the drastic change in dip direction caused the anticlinal highs to now be located on the southeast flanks of these structures. This provides one possible explanation for how and why the Leach Field has some better producing wells off structure to the south and southeast, as seen in Figure 12.

Chapter 6 - Conclusions

Several methods of analysis were conducted on wells of the Leach Field in Jackson County, Kansas in order to better determine the major geologic factors controlling reservoir quality in the Hunton and Viola Limestone Formations. This was done so that a future exploration model can be developed to help increase and stabilize the field's overall production. To better understand the variation of dolomite in the formations, drill cuttings were collected and

thin sections were made for selected wells across the field. These thin sections were analyzed via petrographic microscope to determine porosity type and dolomite crystal attributes such as size and shape. Photomicrographs were taken during the petrographic process so that ImageJ software could be used to calculate and average porosity for each well and formation. Results from the ImageJ process were compared to the results from the petrographic analysis and scanning electron microscope analysis it was determined that the larger the dolomite crystal size, the greater the porosity and permeability observed, resulting in potential for greater fluid low and thus a better producing well. Subsurface mapping was conducted on the field to better determine how the structure of each formation compared to production, as well as reservoir qualities such as dolomitization and porosity. Based on the results it appears that production in the Leach Field can be found in the structural highs of the field, but the largest factor that determines a wells potential is the quality of the reservoir rocks and the degree of dolomitization.

References

Adler, F. J., 1971, Future petroleum provinces of the Midcontinent, region 7; in, Future Petroleum Provinces of the United States--Their Geology and Potential, I. H. Cram, ed.:American Association of Petroleum Geologists, Memoir 15, p. 985-1,120.

Allan, J.R. and Wiggins W.D., 1993, Dolomite Reservoirs: Geochemical Techniques for Evaluating Origin and Distribution, American Association of Petroleum Geologists, AAPG Continuing Education Course Notes, Series 36, 129 p.

Blatt, Harvey, Gerard V. Middleton, and Raymond C. Murray. *Origin of Sedimentary Rocks*. Englewood Cliffs, NJ: Prentice-Hall, 1972. Print

Bornemann, E., Doveton, J. H., St. Clair, P. N., 1982, Lithofacies Analysis of the Viola Limestone in South-central Kansas: Kansas Geol. Survey, Petrophysical Series 3, 50 p.

Caldwell, C. D. and Boeken, R., 1985, Wireline log zones and core description of upper part of the Middle Ordovician Viola Limestone, McClain and McClain SW fields, Nemaha County, KS in Subsurface Geology 6, ed.: Kansas Geological Survey, p. 17-35.

Choquette, P.W., and Pray, L.C., 1970, Geological nomenclature and classification of porosity in sedimentary carbonates: American Association of Petroleum Geologists Bulletin, v. 54,p. 207-250.

Grove, Clayton, and Dougal A. Jerram. "JPOR: An ImageJ Macro to Quantify Total Optical Porosity from Blue-stained Thin Sections."*Computers & Geosciences* 37.11 (2011): 1850-859. Web. 21 Mar. 2016

Hodgden, Jerry H., Robert S. Eaton, and John M. Riley. Production and Reserve Analysis of Leach Field. Denver: Hodgden Oil, 1985, Print.

Jensik, Chandler. Geologic Controls on Reservoir Quality of the Viola Limestone in Soldier Field, Jackson County, Kansas. Thesis. Kansas State University, Department of Geology, 2013 Print.

Lee, Wallace. "The Stratigraphy and Structural Development of the Forest City Basin in Kansas." *Kansas Geological Survey Bulletin 51* (1943), updated 2005: n. pag. *Kansas Geological Survey*. Web. 22 Apr. 2015.

Mishari, A., et. al., 2009, Dolomite: Perspectives on a Perplexing Mineral, Oilfield Review 21, no. 3, 45 p.

Newell, David K., Lynn W. Watney, Stephen W.L. Cheng, and Richard L. Brownrigg. "Stratigraphic and Spatial Distribution of Oil and Gas Production in Kansas." *Kansas Geological Survey, Subsurface Geology Series 9* (1987): n. pag. *Kansas Geological Survey*. Web. 22 Apr. 2015.

Nurmi, R. and Standen, E., 1997, Carbonates: The Inside Story in Middle East Well Evaluation Review, v. 18, p. 26-41.

Scholle, Peter A, and D S. Ulmer-Scholle. A Color Guide to the Petrography of Carbonate Rocks: Grains, Textures, Porosity, Diagenesis. Tulsa, OK: American Association of Petroleum Geologists, 2003. Print.

Warren, J., 2000, Dolomite: Occurrence, Evolution and Economically Important Associations, Earth and Science Reviews, no. 1-3, p. 1-81.

Wells, J. S. "AAPG Datapages/Archives." Petroleum Potential of the Forest City Basin. Tulsa Geological Society Special Publication 3, 1 Jan 1987. Pgs 136-137

Appendix A - Creating Thin Sections

Selecting Samples and Mounting

Step 1 - Warm the hotplate to 250°F placing a plain white piece of paper on top.

Step 2 - Mix Petropoxy® 154 with a 10:1 ratio. (10 parts resin to 1 part curing agent)

Step 3 - Add 3 drops blue dye to resin. This will help determine porosity using ImageJ software.

Step 4 - Fully submerge drill cuttings in cup of mixed blue dye and epoxy. Place vacuum bell jar over top and vacuum for 1-2 minutes. Periodically releasing pressure to allow epoxy to fill void spaces.

Step 5 - Place well cuttings on clean/dry glass slide, align cuttings to have the most surface are glued directly to the slide.

Step 6 - Cover cuttings in a few drops of epoxy. (Trial and error proved that the best amount is to just cover the cuttings, too much will cause the slide to break as epoxy hardens)

Step 7 - Place glide on double sided tape, this will keep sample from moving while under vacuum pressure.

Step 8 - Place glass slide under bell vacuum jar and vacuum for vacuuming out air to remove bubbles from epoxy. Vacuum samples for 1-2 minutes.

Step 9 - Remove slide from vacuum chamber and place on plain white paper then place on top of the hotplate for 10 minutes.

Step 10 - Unplug hotplate after 10 minutes and allow thin section to cool overnight to ensure epoxy has set up fully.

Step 11 - Sand down thin section on brass wheel grinder to approximately 30 microns, checking periodically with backlit microscope to ensure cuttings appear translucent and are not being ground off.

Step 12 - Polish samples on a water-cooled thin section polishing machine using silicon carbide sandpaper. For best results use increasingly finer paper beginning with 1000 grit and moving on to 2000, and 2500 grit.

Step 13 - Check thin section under petrographic microscope to ensure good visibility of cuttings.

Selecting and Mounting Samples

Figure 21 - A) Samples in box; B) Cuttings from bag; C) Corvascope setup; D) Epoxy and blue dye; E) Slide with cuttings and epoxy; F) Vacuum chamber with slide inside; G) Hotplate with plain white paper on top
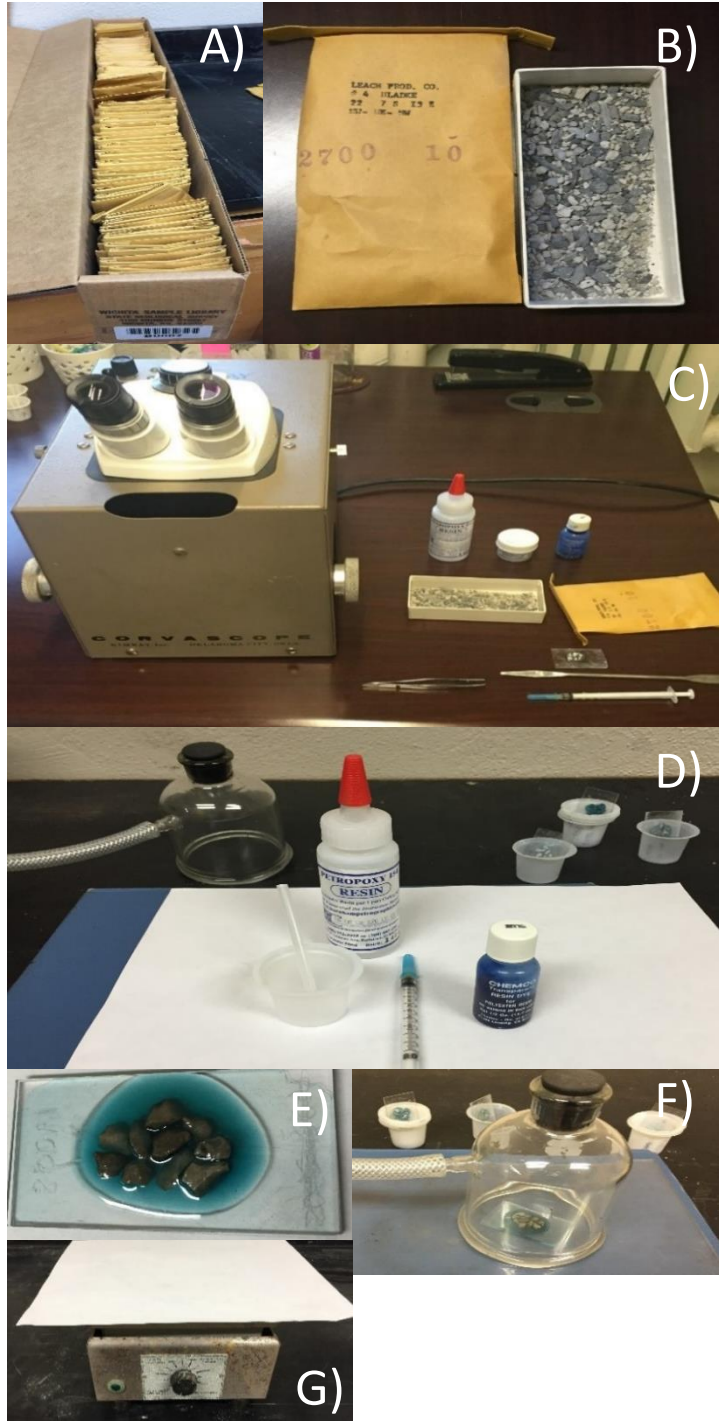
Grinding and Polishing Samples

Figure 22 - A) Water cooled wheel grinder; B) Sample in holder; C) Brass wheel; D) Thin section polisher; E) Thin section sample holder; F) Sample being polished; G) Finished samples in cups for organization.
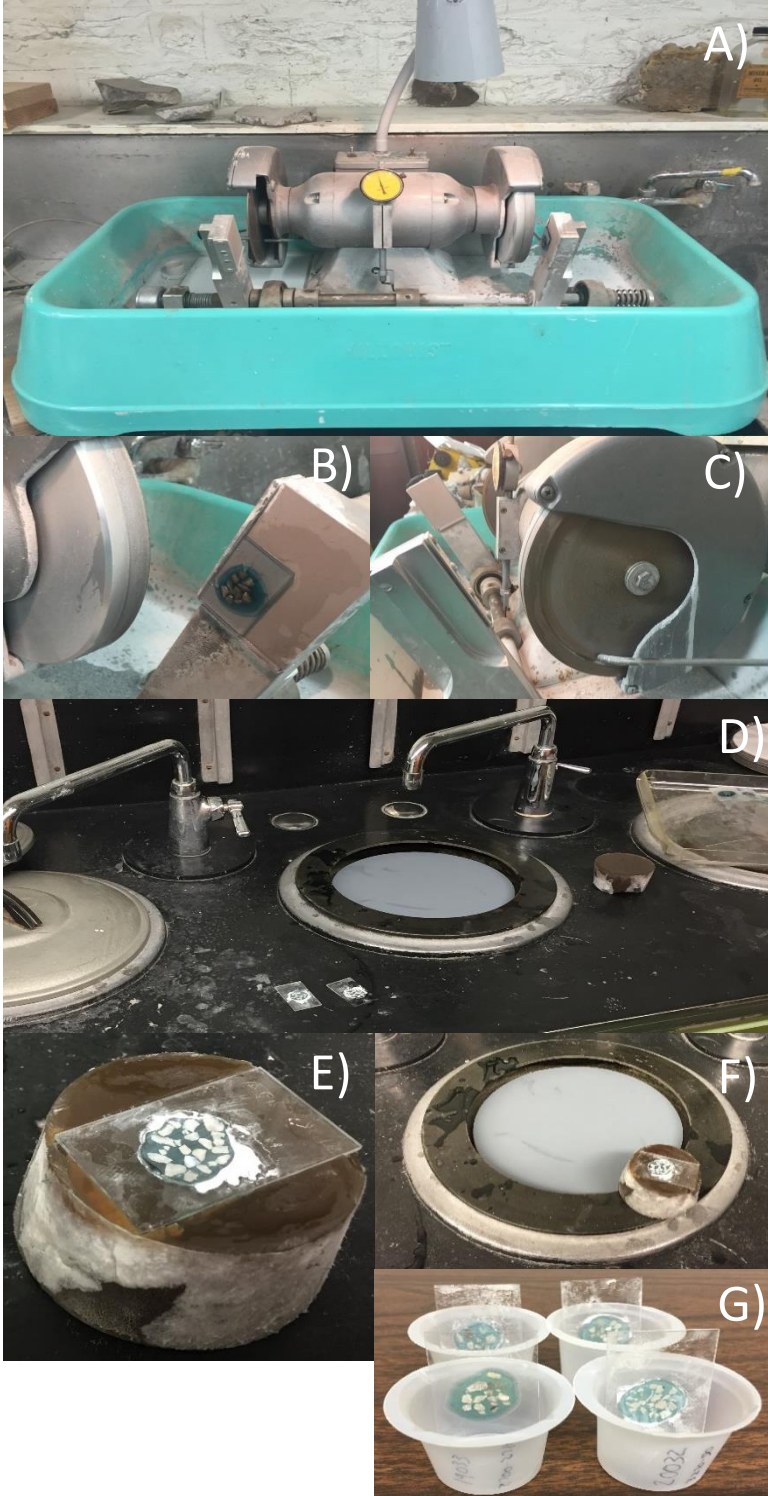
Appendix B -

ImageJ Porosity Calculations

Preparing Images

The steps to get a digital image into an 8-bit paletted .bmp file are as follows (Grove & Jerram, 2011).

1. Open image in Adobe Photoshop.

2. Crop image only comprising the sample. Making sure to use the same image size throughout for each of the samples.

3. Convert cropped image to an 8-bit palette file by using jPOR_60 palette.

   a. "Image > Mode > Indexed Color. Set "Palette" to "Custom" and you will be presented with a new window—click load and navigate to the custom JPOR palette (JPOR_60) and click load—OK this operation. Set dither to none under Indexed Color options and click OK. The image will now be an 8-bit palette file. This can be automated by recording the action then playing it via the Automate > Batch tool," (Grove & Jerram, 2011).

Save the image as a .bmp file.

Using ImageJ

The steps to calculate porosity using the jPOR Palette in ImageJ are as follows (Grove & Jerram, 2011).

1. Right click saved .bmp file and open it using ImageJ.

2. This will open up the image into a new window within ImageJ and it will also prompt you to start porosity measurements by pressing F1.

3. "Pressing F1 automatically thresholds the image using the default values, and displays the threshold command box where the threshold level can be manually adjusted to refine the porosity selection," (Grove & Jerram, 2011).

4. Once the porosity is selected press F2.

5. This calculates the area of thresholded pixels within the images, meaning it calculates the area of color pixels that are within the selected threshold range, and gives the of porosity value as a percentage.

6. To avoid recalculating the porosity and to end the batch, press F5